MELİKŞAH ÜNİVERSİTESİ
KAYSERİ

The Graduate Institute of Science and Engineering

M.Sc. Thesis in Material Science and Mechanical Engineering

Effect of Boron on the Mechanical Properties of High Strength Low Alloy AISI 4140 Steel

by

Bashir Idris Rabiu

July 2014
Kayseri, Turkey

Effect of Boron on the Mechanical Properties of High Strength Low Alloy AISI 4140 Steel

By

Bashir Idris Rabiu

A thesis submitted to

the Graduate Institute of Science and Engineering

of

Meliksah University

in partial fulfillment of the requirements for the degree of

Master of Science

in

Material Science and Mechanical Engineering

July 2014
Kayseri, Turkey

APPROVAL PAGE

This is to certify that I have read the thesis entitled "**Effect of Boron on the Mechanical Properties of High Strength Low Alloy AIS I4140 Steel**" by Bashir Idris Rabiuand that in my opinion it is fully adequate, in scope and quality, as a thesis for the degree of Master of Science in Material Science and Mechanical Engineering, the Graduate Institute of Science and Engineering, Melikşah University.

_____

Prof. Dr. M. HalidunKeleştemur
Head of Department

I certify that this thesis satisfies all the requirements as a thesis for the degree of Master of Science.

_____

Prof. Dr. M. HalidunKeleştemur
Supervisor

Examining Committee Members

Title and Name		Approved
Asst.Prof. Dr.Ercan SEVKAT	July 24, 2014	_____
Prof. Dr. M. HalidunKeleştemur	July 24, 2014	_____
Asst.Prof. Dr. Gökhan ÖZGÜR	July 24, 2014	_____

It is approved that this thesis has been written in compliance with the formatting rules laid down by the Graduate Institute of Science and Engineering.

_____

Prof. Dr. M. HalidunKeleştemur
Director

July2014

Effect of Boron on the Mechanical Properties of High Strength Low Alloy AISI 4140 Steel

Bashir Idris Rabiu

M.S. Thesis in Material Science and Mechanical Engineering

July 2014

Supervisor: Prof. Dr. M. HalidunKeleştemur

ABSTRACT

This work describes the effect of boron additions on the mechanical properties of a high strength low alloy AISIS 4140 steel with boron content 2.1ppm, 11.4ppm, 17.2ppm, 25.6ppm, 31.7ppm and 37.7ppm manufactured by hot rolling as-received, after normalization and cool in air, water and oil quenched at temperature of 850°c, 860°c, 880°c, 900°c, 960°c and 1000°c. The manufacturing process of the steel promotes the formation of martensite and retained austenite in the as-cast state. The steel hardness has the maximum hardness for the boron content of 2.1ppm and 25.6ppm, and reduces linearly for the others in the as-cast state, and also for the normalized steel the hardness value increases with decrease in temperature and an increase in boron content, but not linearly at some boron content. The hardness starts increasing as the boron content increases up to 17.5ppm, but drops at the highest boron content with the maximum and minimum hardness at 17.5 and 31.7ppm. The decrease and increase in the hardness of the steel is due to the phase transformation and precipitation behavior of boron. Furthermore, the wear resistance increases and then decreases with increasing boron content.

Keywords: AISI 4140, Steel with Boron, Normalization, Heat treatment, Wear, Bainite, Martensite

Effect of Boron on the Mechanical Properties of High Strength Low Alloy AISI 4140 Steel

Bashir Idris Rabiu

Yüksek Lisans Tezi, Malzeme Bilimi ve Makine Mühendisliği

Temmuz 2014

Tez Yöneticisi: Prof. Dr. M. HalidunKeleştemur

ÖZET

Bu çalışma sıcak haddeleme işlemi ile şekilllendirilmiş, normalizasyon sonrası 850 ^{o}C, 860 ^{o}C, 880^{o}C, 900^{o}C, 960^{o}C ve 1000^{o}C'de tavlanıp hava, su ve yağ atmosferinde soğutulan 2.1ppm, 11.4ppm, 17.2ppm, 25,6ppm, 31,7ppm bor ilaveli, düşük alaşımlı SAE 4140 çeliğinin, mekanik özelliklerini araştırmak için gerçekleştirilmiştir. Çeliğin imalat prosesi döküm yapısında kalıntı östenit ve martenzit oluşumunu teşvik eder. Lineer olarak azalan çeliğin sertlik değerleri 2.1pp ve 25.6pp bor ilavesi için maksimum sertliktedir ve normalizeli çeliğin sertlik değerleri azalan sıcaklık ve artan bor ilavesi ile artmaktadır ancak bazı boron içeriklerinde lineer değildir. Su ortamında sertleştirilmiş ısıl işlemli ve sertleştirilmiş çeliğin sertlik değerleri, yağ ortamında sertleştirilmiş çelikten daha yüksektir (55-59 HRC su, 51-54 HRC yağ). Bunun dışında aşınma direnci bor oranının artması ile başlangıçta yükselir ancak belli bir bor oranından sonra düşer. Yapılan mikroskobik çalışmlarda çeliğin ısıl işlem proseslerinde homojen olmayan mikroyapı yapının mevcut olduğu gözlenmiştir.

Keywords: AISI 4140, Çelik ve Bor, Normalizasyon, IsılİşlemAşınma, Beynit

DEDICATION

I dedicate this thesis to my parents for their tireless, indefatigable and earnest support, love, and encouragement they have been offering me since childhood to where and how I am today. My achievements in life wouldn't have been materialized without their prayer, guidance and the philosophy of hardworking they imparted on me.

ACKNOWLEDGEMENT

Without the meaningful suggestions and advice from my supervisor, whose strenuouspassion for software verification strengthens my enthusiasm for my research area, this thesis wouldn't have go beyond a mere dream.My sincere appreciation goes to my thesis supervisor and also course instructor Prof. Dr. M. HalidunKeleştemur

I remain grateful to His Excellency, the Executive Governor of Kano State-Nigeria, Engr. Dr. Rabi'u Musa. Apart from the knowledge acquired, this has given me an opportunity to explore other part of the world.

I also express my earnest indebtedness to my H.O.D and course instructor, Prof. Dr. M. HalidunKeleştemur together with the encourage of academic staffs of my department for all the support and the knowledge they imparted to me and to my lab colleague Hasan Yeşilyurt for his great support. This has contributed immensely while carrying out this research.

I similarly owe a great deal of thanks to my brothers, sisters, uncles, friends and most importantly 18 M.Sc. students with which I benefited the 501 Kano State Scholarship Scheme.

TABLE OF CONTENTS

LIST OF TABLES

LIST OF FIGURES

CHAPTER 1

INTRODUCTION AND LITERATURE REVIEW

1.1 INTRODUCTION

The request for steels with high toughness, high strength, and outstanding welding properties for transportation systems and energy conversion has led in recent years to the development of different classes of HSLA steels. Boron occupies an important place in this context because it can substitute expensive alloying elements. The influence of boron alloying on the microstructure of alloys other than steel, such as nickel base alloys has been described by various authors and it was found that boron containing nickel alloys were less susceptible to environmental degradation of mechanical properties by grain boundary attack. It was also observed that the high temperature mechanical properties of a polycrystalline nickel base super alloy can be advance by small additions of boron and carbon [1- 4]. Boron has been added to steels to advance their strength since the 1970's. The addition of boron essentially is to promote bainite and martensite formation by suppressing the austenite alteration (i.e.to increase the hardenability of the steels) [1- 4]. It is observed that boron has to remain in solid solution in order for its hardenability to be kept active. Carbide formers and nitride such as Ti and Nb are added to boron steel so as to bonds nitrogen and carbon in the steels and hence protecting boron from forming Fe_{23} $(B, C)_6$ or BN. Residual boron in solution is capable of segregating at the austenite grain boundaries and then occupy ferrite nucleation sites, henceforth promoting bainite and martensite formation by delaying ferrite formation [4-7].

Additionally, at the austenite grain surface there is a delay of the heterogeneous nucleation of ferrite due to boron, which in turn enhances the hardenability of the steel. It is more likely that the segregation of boron to the grain boundaries is due to the decrease in

the interfacial energy. This makes the gain boundaries less active as heterogeneous site. Though boron effect on steel is completely different in plain and alloyed steel, low and high carbon steel, additionally the effect is also affected with low and high waiting time, with low and high soaking temperature, and with low and high cooling rate due its precipitate formation [8]. However, the mechanism by which boron additions enhanced high temperature mechanical properties is less clear and it is observed that extreme boron additions enhanced ductility at the expense of creep strength and intergranular fracture, lower amounts of boron produced creep strength by reducing the rate of void development on those grain boundaries which were transverse to the applied stress [9]. At the austenite grain boundaries the dominating presence of boron has been revealed experimentally that only the dissolved boron exerts a promising effect on the hardenability, and the concentration of boron in the solid solution should be at least 0.0008% for the hardenability to increase [10]. Also the hardenability produce by about 0.9%Cr, 3.2% Ni or 0.7% Mo can be achieved by the increased addition of only 0.0005 to 0.003% boron to 0.2% carbon steel. It is also seen that in steel, an increase up to the eutectoid composition in carbon content decreases the boron hardenability factor linearly [11]. It is found that with the addition of 15 to 25 ppm of boron optimum combination of hardenability and toughness can be achieved [12]. And it was also shown that by alloying 1.0% Cr and 0.7% Mn with 20 ppm of boron, optimum tensile strength results can be achieved [13]. Although boron steel was designed mainly for the hard and wear–resistant element, now they are also designed for wider application. In this research study, we examine the normalization, oil and water quenching effect on AISI 4140 boron containing steel produce by a company in Turkey. The steel was supplied by the manufacture after hot rolling to be heat treated in a suitable manner by the purchaser. Six AISI 4140 steels with different boron content, within 2.1ppm -37.7ppm, were studied.

1.2 BORON STEEL

1.2.1 Development of Boron Steel

In 1907, boron was primarily considered as a possible alloying element in steel [1]. Additionally, it was recognized in 1921 that boron up to 2 weight% in some steels makes the steels extremely brittle and hard, though this amount of boron is now considered to be extremely high [2,3].Through 1930's and early 1940's a substantial number of research regarding the influence of alloying elements on the hardenability of steels were performed[4-6]. Boron was accepted as the strongest hardenability agent among the other alloying elements. The slow commercialization of boron containing steel is caused by the failure to control the boron content precisely during the steel making process and the lack of understanding on the hardness of boron containing steels. The true commercial development of boron steel began during the Second World War. Classical hardenability alloy elements, such as nickel and chromium shortage, made an opening for boron to be the alternative as an alloying elements. Boron seemed to be a very favorable alternative alloying element in steel, although due to the limitations of steel making techniques during the Second World War makes the full use of boron steel products very slow, because keeping boron in the solution was the key problem. During boron steel production, due to greater affinity of boron with oxygen and nitrogen, proper controlled of these two elements must be ensured before boron is added during the steel production process. Allowing the combination of boron with oxygen and nitrogen at an early stage of the steel making process causes decrease in the effectiveness on steel hardenability. Protecting boron from forming boron-nitride (BN), boron-oxide (B_20_3), and iron boron-carbide [Fe_{23}(C,B)6] or boron-cementite [Fe_3 (C, B)] in the earlier years, was a problem faced by melting shops due to the difficulty of keeping boron in a solution [7]. The adding of deoxidizers, aluminum and silicon, with the development of steelmaking technology, as well as other stronger nitride formers such as zirconium and titanium were used to clean up the steel for boron addition.

Kapadia and coworkers in 1968 introduced an empirical formula, given in equation 1.1 [14].

$$ß = \{B-[(N-0.002)-Ti/5-Zr/15]\} \quad \text{---------- 1.1}$$

ß represents the actual boron content which is accountable for the hardenability of steels. It can be understood that this equation qualitatively reflects the preceding remarks.

Addition of boron into low carbon Microalloyed steels has been in existence since 1970's. With the improvement of the advanced analytical equipment's today, they have been far better understanding of the effects of boron. Steel making techniques today have made it possible to carefully control the effective boron content in steel. Therefore, the main properties of boron containing steels can be achieved frequently.

1.2.2 Effect of Composition in Boron Containing Steel

1.2.2.1 Alloying Elements

The strength of a steel is increased by boron addition which in turn promotes bainite and martensite transformation. It was also found that the addition of certain alloying elements improves the effect of boron on strengthening. For example, the existence of molybdenum strongly improves the effect of boron [15]. Though vanadium has a well-known influence to precipitation hardening, it has very little influence on the steel with boron. Additionally, niobium advances the boron effect extraordinarily when it is in solution [16]. It was also seen that there is a significant drop in the transformation temperature of austenite to ferrite when copper and boron are combined. Alternatively, the austenite crystallization kinetics can be affected by the addition of boron in steel. By means of a multiple- hot torsion simulation, Bai studied widely the effects of alloying composition and process parameters on the non-crystallization temperature [17]. It was also seen in his work that compared to a plain carbon steel, the non-crystallization temperature (T_{nr}) increases with boron additions. Conversely, it was seen in a Nb-B steel that they have a more significant increase in the non-crystallization temperature. The effect of different alloy combinations on the recrystallization finish temperature was also investigated by Tamehiro [18].

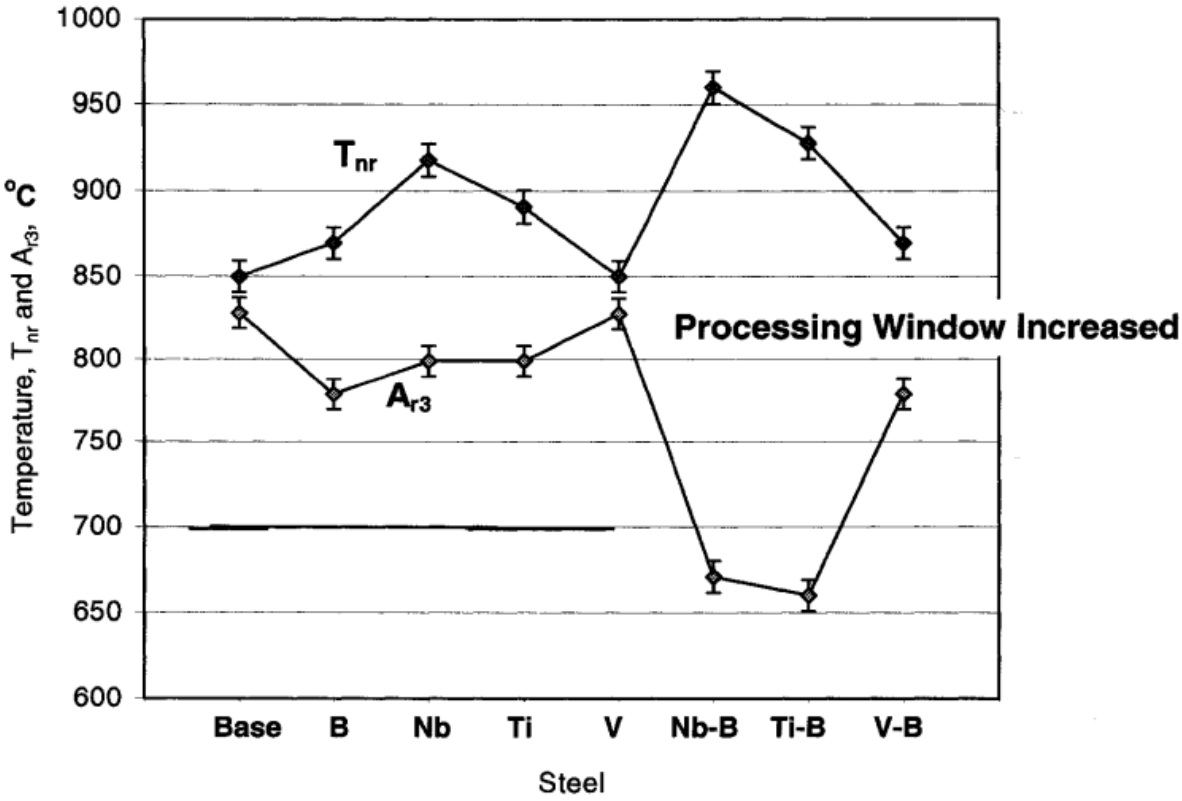

Figure 1.1 Schematic diagram showing processing windows for steels with boron additions and microalloying [18].

The strongest alloying element which slows down austenite recrystallization among the studied microalloying elements is Nb as can be seen in figure 1.1 and leads to a substantial growth in the recrystallization finish temperature compared to the base steel (plain carbon). More increase in the recrystallization finish temperature and a wide processing window for control rolling or pancake rolling can be achieved by a combined addition of Nb-B in steel. The possibility that boron atoms accelerate the diffusivity of these alloying elements in austenite may be the mechanism responsible for increasing the non-recrystallization temperature. Henceforth, it leads to more rapid precipitation kinetics, and supports Nb(C,) precipitation at higher temperatures. Otherwise, the boron atoms might slow down grain boundary motion, letting precipitates to form more easily on grain boundaries. The movement of the austenite grain boundaries can be pinned by

these high temperature precipitates, and therefore led to a higher non-crystallization temperature (T_{nr}) and stop austenite recrystallization.

1.2.2.2 Carbon level

The steel with high alloying elements, particularly high carbon level, decreases the effectiveness of boron [7]. In the late 1940's, the boron effect of different types of commercially produced low alloy and plain carbon steels was studied by Rahrer and Armstrong [7]. The amount of carbon in the examined steels varied from 0.1wt% to 1.0wt%. They concluded in this earlier study that the boron effect on the hardenability of steel reduced with increasing carbon level in the steel. The equation 1.2 can be used to determine the effect of boron:

$$F_{ß} = 1 + 1.5\ (0.9 - \%C) \quad \text{---------- 1.2}$$

$F_{ß}$ is the hardenability factor of boron. From equation 1.2, it can be seen that boron is ineffective for steels with carbon level higher than 0.9 weight percent. Hayes had similar results based on the hardenability evaluations of heat treated low carbon alloy steels, but with a slightly steeper linear relationship [19]. Currently low-alloy and high-carbon steels used for sheet and strip are replaced by available low-cost low carbon, boron-containing steels. Due to the better cold-forming characteristics of low carbon boron-containing steels makes it able to be heat treated to comparable hardness and greater toughness for a wide variety of applications, such as machine components, tools, and fasteners. Boron effect on the steel hardenability varies particularly with the carbon content of the steel which makes boron to be usually added to low or medium carbon steels. Because, the effect of boron is much less in high carbon steels, also the complete effect of boron on steel hardenability can be attained only in fully deoxidized or aluminum-killed steels. For an optimum hardenability effect, only 0.001% boron is required when an appropriate protection of boron is afforded by additions of zirconium or titanium [19].

1.2.3 Effect of Boron on Mechanical Properties

1.2.3.1 Hardenability of boron steel

As well known before that the addition of boron can remarkably increase hardenability of a steel [14-15, 20-20]. The hardenability of the steel can be enhanced with an addition of only 0.0010 - 003% soluble boron to a suitably protected base steel, up to a level equivalent to that obtained by adding about 0.5% manganese, molybdenum or chromium. Concerning the effect of boron, a lot of researches have been done on the austenite to ferrite transformation. Boron can retard the nucleation rate of ferrite since ferrite usually nucleates on the austenite grain boundaries by segregating to the austenite grain boundaries [26]. Two reasons basically are responsible for such a robust suppression of ferrite formation with such a minute boron content. Firstly, because of the low atomic weight of boron compared to that of iron and secondly 10 ppm boron by weight of solute boron is truly equals to 52 ppm atoms. Assuming that this boron goes to grain boundaries, it has been estimated that 4 billion boron atoms are present for every ferrite nucleus for an austenite grain size of 30μm [27].

1.2.3.2 Other Mechanical Properties of Boron Steel

- **Hot Workability and Creep Rupture Life**

It has been investigated that suitable amounts of boron (0.002 - 0.005 %wt) enhances the creep rupture life of austenitic stainless steels [18, 28]. Boron was proved to have a beneficial effect on the creep properties of ferritic steels in combination with Mo,Ti or Nb in the mid-70s [30]. Recently, there was also a confirmation in the enhancement of the creep rupture life of 9Cr-3W-3Co-NbV steels by the addition of boron [29]. The hot workability of steels is enhanced also by addition of boron when it substitute other alloying elements such as V, Cr,Nb, and Mo at high hot working temperature as the precipitation strengthening effect on austenite is minimized [6,31].

1.2.4 Grain Boundary Segregation of Boron

The inherent inhomogeneity of interfaces determines primarily the mechanism of segregation to that interfaces. A narrow zone of segregation is formed due to the accumulation of impurity atoms at grain boundaries and surfaces. An isotropic bulk solid

may change locally into a highly anisotropic medium as a result of the sharp concentration gradients. At the grain boundary small bulk concentrations of impurity atoms can lead to substantial amounts of those atoms, which can significantly change the mechanical properties of the steel. The segregation of solute atoms at austenite grain boundaries can be classified into equilibrium and non-equilibrium segregation. The thermodynamics and isothermal kinetics theories of equilibrium segregation have been studied in detail elsewhere [32-34]. Equilibrium segregation is a thermodynamic process and happens mainly during the isothermal holding of the material at a certain temperature. Non-equilibrium segregation is a kinetically dependent process and occurs during the cooling of material from a higher temperature. It increases with increasing cooling start temperature for the same cooling rate and decreases with increasing cooling rate at the same cooling starting temperature [36, 37]. Westbrook clarified the non-equilibrium segregation of boron to grain boundaries as he detected a hardness increment at grain boundaries in a few quenched and dilute non-ferrous alloys [35]. The study of the influence of hot rolling and heat treatment on boron segregation in steel was carried out by some researchers in the early 1980's [38]. It was suggested that the bulk diffusion of boron atoms,the sweeping velocity of recrystallizing austenite grain boundaries and the grain boundary diffusion of boron atoms determine the segregation behavior of boron atoms during hot rolling. More recently, further investigations of non-equilibrium boron segregation behaviors were performed [39]. The higher the cooling start temperature, the higher the segregation for a given cooling rate. Also the lower the cooling rate, the larger the segregation level for the same cooling starting temperature.

1.2.5 Boron in Low Carbon Micro Alloy Steels

As previously mentioned, it is well known that boron significantly improves the hardenability of steel by suppressing the austenite to ferrite transformation. Therefore, higher strength can be obtained by the formation of bainite or martensite in such way. Often, a notable reduction in toughness is connected with the formation of these hard microstructures. The effective grain size for cleavage fracture of bainitic steels was founded by Pickering that it depends strongly on the austenite grain size prior to

transformation [40]. So,it is necessary to minimize the size of austenite grains prior to the bainite transformation in order to enhance the toughness of the steel. Modern bainitic steels for structural applications generally have very low carbon contents less than 0.05%wt and are Microalloyed, as such the lower carbon level in this steel makes it to have good weldability. The combination of micro alloying elements, such as Nb, V, and Ti with boron makes a wide processing window for pancake rolling to be obtain. So, a substantial total reduction below the Tnr, but in the single phase austenite region, is possible, which through the microstructure refinement generally improves the steel toughness.

1.2.6 Time Temperature Transformation (TTT) Diagram

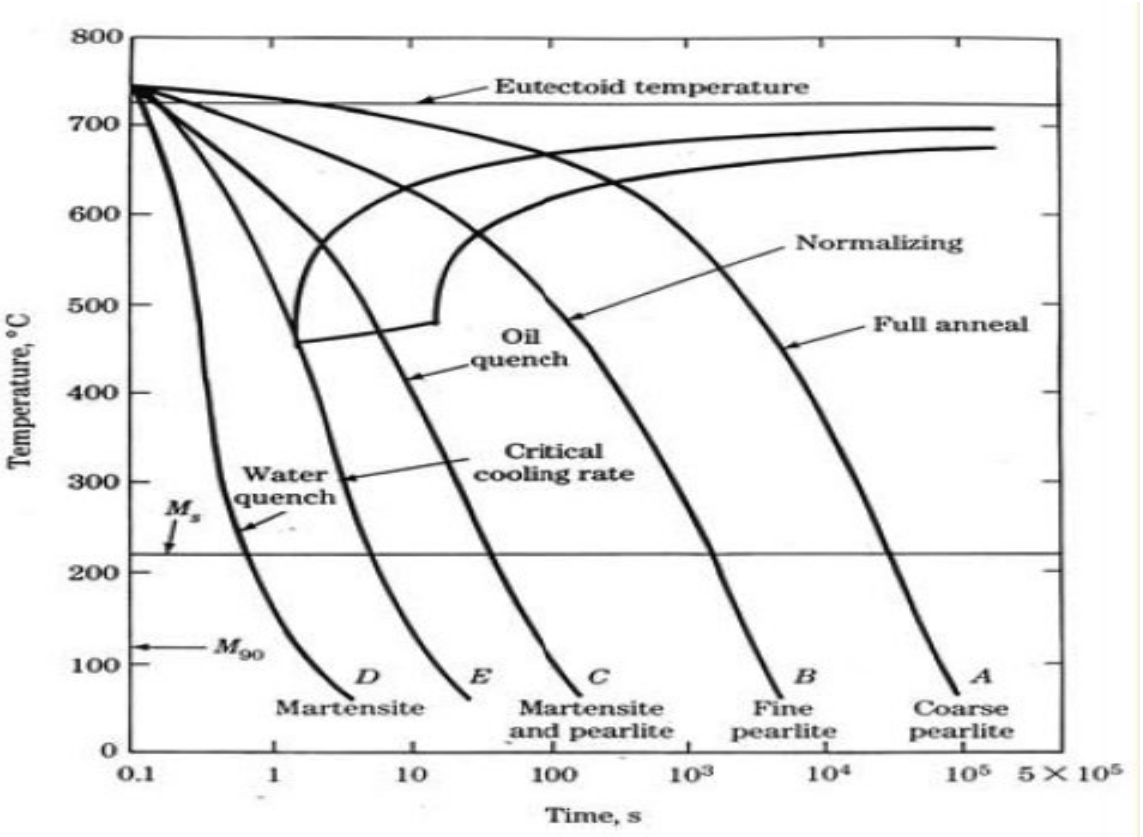

Figure 1.2. TTT diagram showing cooling part A-D for a plane carbon steels.

Figure 1.2 shows five cooling paths A through D. Each line indicates a different cooling rate and therefore different resultant steel structure. Steels with less than 0.3 %

carbon cannot be hardened effectively, while the maximum effect is obtained at about 0.76 % due to a decreased tendency to retain Austenite in high carbon steels [41].

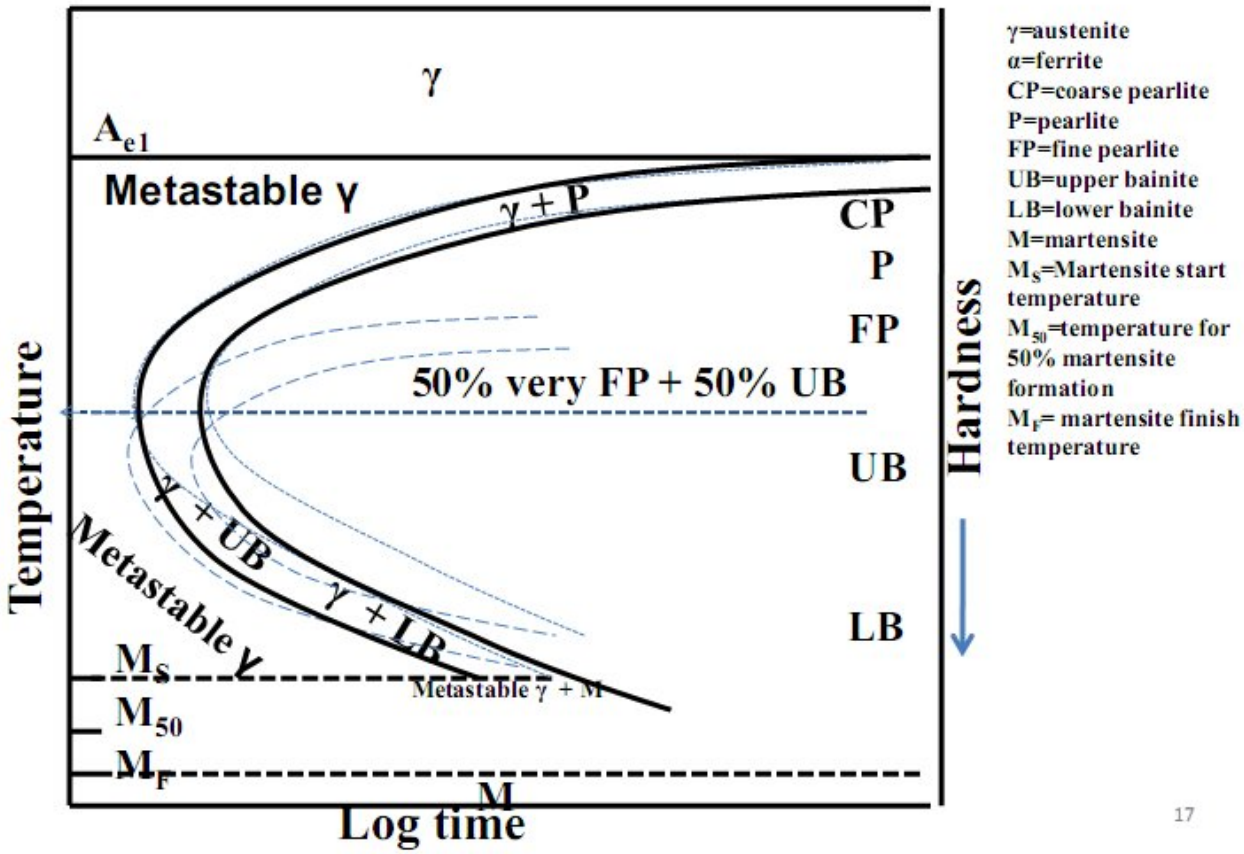

Figure. 1.3: Time Temperature Transformation (schematic) diagram for plain carbon eutectoid steel.

Figure. 1.3 shows the temperature transformation for plain carbon eutectic steel and the region for formation of different type of ferrite and bainite.

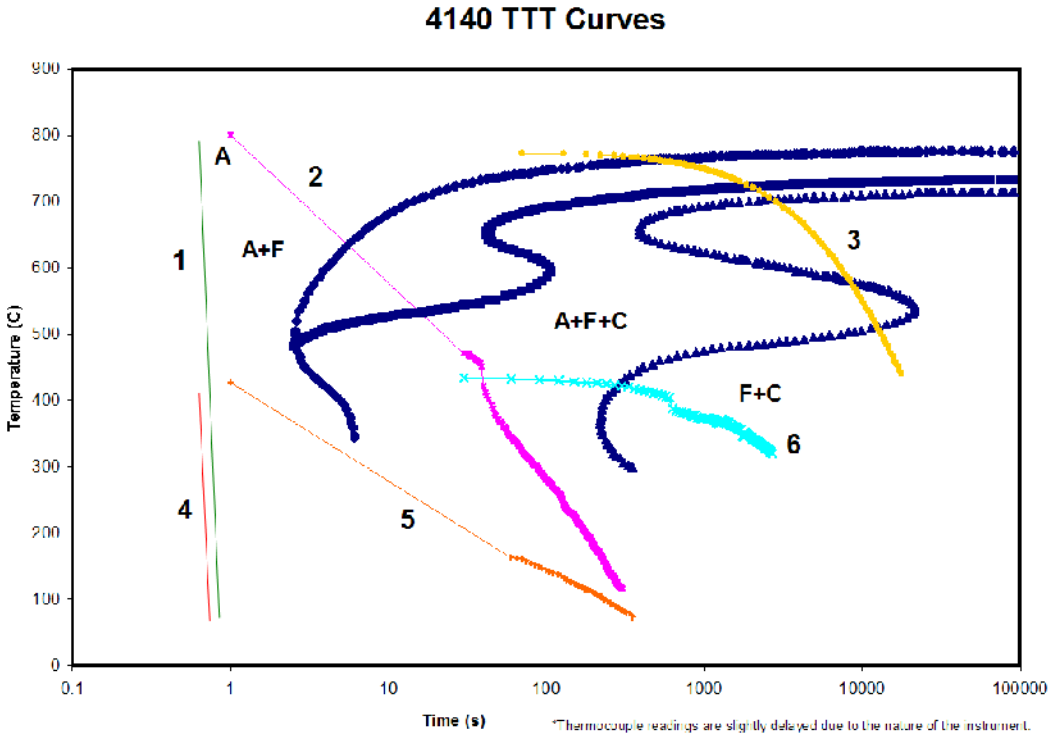

Figure 1.4 TTT diagram for 4140 steel [43].

Table 1.1 hardness value for 4140 steel [43].

Time held at 800C	Rockwell Hardness Test (C)			
Normalize in air 8 hour	34.5	34	34.5	34
1 hour	30.5	31.5	30.5	32
Quenched 8 hours	49	52	52	51
1 hour	38	38	41	40.5

Figure 1.4 shows the time temperature transformation diagram for AISI 4140 steel without boron addition which shows more chances of ferrite formation within the austenite region. And **Table 1.1** shows the hardness value for 4140 steel without boron addition which shows lower hardness values compare to that with boron, as can be seen in **table** 3.1, 3.2 and 3.3 due to difference in transformation phases of the TTT diagram.

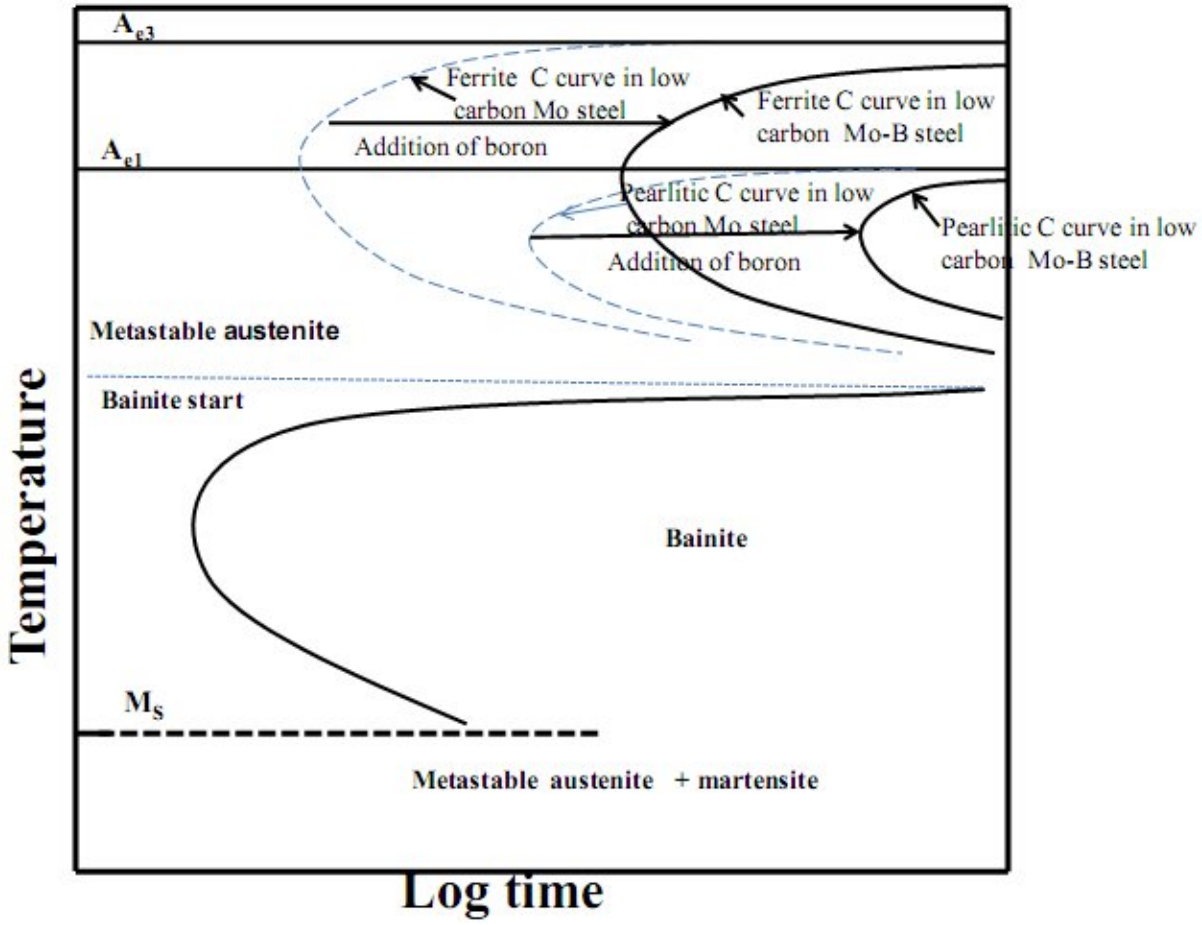

Figure. 1.5: Effect of boron on TTT diagram of low carbon Mo steel.

In figure. 1.5 It can be seen that the addition of alloying elements leads to a greater separation of the reactions and result in separate C-curves for pearlitic and bainitic regions. Mo encourage bainitic reaction but addition of boron retard the ferrite reaction. By addition of B in low carbon Mo steel the bainitic region which is almost unaffected by addition of B can be separated from the ferritic region [42].

1.2.7 Calculation of TTT Diagram of 4140Steel

Substantial work has been embarked on to develop material models that can calculate CCT diagrams and TTT for steels, and now for a wide range of steels such calculation can be performed, such as tool steels, medium to high alloy types, and stainless steels [44].

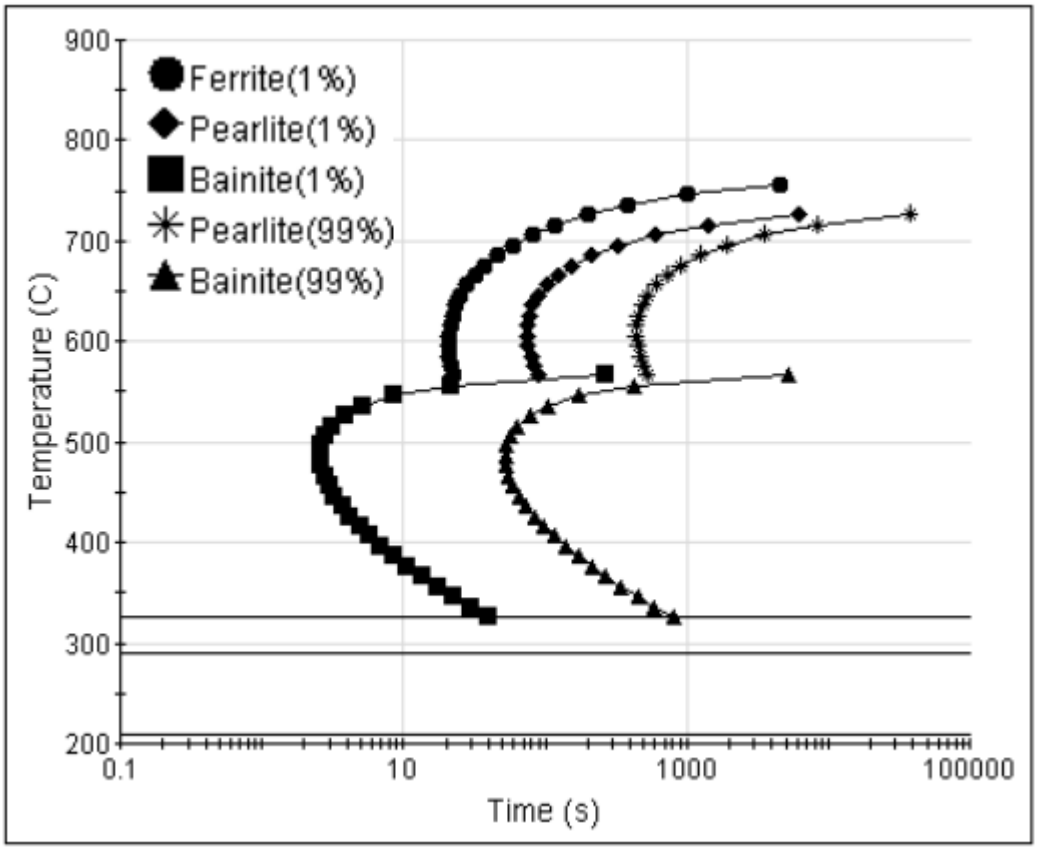

Figure 1.6. Calculated TTT diagram of steel 4140 [45].

The current model is based on a former model proposed by Kirkaldy etal for the transformation from austenite to ferrite, pearlite and bainite [45]. It takes on the equation 1.3 form, which calculates the time (τ) to transform x fraction of austenite at a temperature T.

$$\tau(x,T) = \frac{1}{\alpha D \Delta T^q} \int_0^x \frac{dx}{x^{2(1-x)/3}(1-x)^{2x/3}} \quad \text{---------- 1.3}$$

where $\alpha=\beta 2^{(G-1)/2}$, G is the ASTM grain size, β is an empirical coefficient, D is an effective diffusion coefficient, q is an exponent dependent on the diffusion mechanism , and ΔT is the undercooling. **Figure 1.6** shows the CCT diagram which is obtained after the TTT diagram has been calculated, using well-established additivity rules [45].

Because of the huge volume change associated with this transformation a correct description of the martensitic transformation is of great significant. The amount of martensite, f_M, as a function of the undercooling ΔT below martensite start temperature Ms is calculated using the equation 1.4 [46].

$$f_M = 1 - \exp(-c \cdot \sqrt{Ms} \cdot \Delta T) \text{----------} \quad 1.4$$

CHAPTER 2

MATERIALS AND EXPERIMENTAL PROCEDURE

2.1 MATERIALS

In this study, effect of boron addition on microstructure and some of mechanical behavior was investigated in the AISI 4140 steel which is studied in Nevsehir University, Turkey. The investigation was carried out so as to determine the mechanical properties after different heat treatment. The Chemical composition of the investigated steel is summarized in the table 2. This composition is selected not only because of the need to obtain relatively high mechanical properties, but also must be to ensured its weldability for the apply universitility.

After the melting process of the AISI 4140 steel in a 35 kg melting capacity non-vacuum induction furnace at 1635ºC, the pearlite powder was applied to the liquid material and a thin layer of slags was formed on the surface. The layer created by the pearlite powder was taken out with a cold metal rod from over the melt while adding aluminum, titanium and boron and during the casting process. Thanks to this process, the mixture of oxygen and nitrogen to the melt in the non-vacuum induction furnace from the air was kept at the minimum level. The melt was cast in square-shaped ceramic molds in 30x30 mm thickness heated until 450ºC and it was cool in the air. The obtained square-shaped materials at 30x30 mm in size were kept at 1200 ºC for 60 minutes in the furnace in the laboratories, and they were exposed to deformation at 80% by rolling them at two passes in a hot rolling device with brand of HILLE. The hot deformation's second rolling out pass temperature was given close attention to be in the austenite (950 ºC) region. The additional detail of this procedure is given elsewhere [50].

Table 2.1. Comparison of chemical analyses of AISI 4140 steel containing boron in different ratios by weight %

B	2.1ppm(11)	11.4ppm(12)	17.2ppm(13)	25.6ppm(14)	31.7ppm(15)	37.7ppm(16)
Si	0.18295%	0.18629%	0.17994%	0.17317%	0.16967%	0.15639%
Mn	0.83752%	0.84588%	0.82236%	0.79682%	0.79015%	0.76518%
P	0.01339%	0.01516%	0.01432%	0.01145%	0.01375%	0.01338%
Cr	0.87773%	0.88739%	0.87559%	0.86454%	0.86932%	0.87540%
Ni	0.04856%	0.04850%	0.04822%	0.04773%	0.04827%	0.04845%
Cu	0.06337%	0.06517%	0.06306%	0.06342%	0.06314%	0.06448%
Ti	0.02786%	0.02520%	0.02100%	0.01956%	0.01730%	0.01400%
N	0.01260%	0.01369%	0.01230%	0.01285%	0.01120%	0.01200%
C	0.44102%	0.43944%	0.43898%	0.44141%	0.44686%	0.44292%
V	0.00630%	0.00658%	0.00621%	0.00599%	0.00596%	0.00599%
Nb	0.00296%	0.00326%	0.00298%	0.00307%	0.00305%	0.00317%

2.2 EXPERIMENTAL EQUIPMENTS

The heat treatment furnace with a temperature up to 1200^0C, Protherm Furnace Model: PLF 120/10, was used for the different kinds of heat treatment work.

The hardness measurements were made using a test machine UHT-900D motorized Brinell, Rockwell and Vickers hardness tester, under a load of 150kg and a diamond indenter. Three hardness readings were recorded and the average reading using Rockwell (HRC) is reported here.

Optical microscopy was performed on a Nikon optical microscope (EPIPHOT 200) in order to reveal the details of the microstructure, the samples were mounted, grind and polished in the standard manner for the basic metallography's characterization. The polished samples were etching with 5% nital to reveal the microstructure and the etching time was about 10 to 15 seconds. All samples were examined at magnifications of 200X and 400X.

Under these magnifications, not much details of the microstructures reveals. However, there is still much valuable information on the morphology of the microstructures, grain boundaries, and second phases, etc. that can be obtained from these optical observations.

The wear test was performed using a nanovea tribometer, **figure 2.2** (a), which uses a rotative and linear modes on a single system and offers specific and repeatable wear and friction testing. At the core the nanovea tribometer is designed with a high quality motor and a 20bit position encoder. The speeds of the tribometer ranges from 0.01 to 2000rpm. A series of step speeds can be run continuously during the tests because the tribometer has a full and precise control of its motor.To achieve a controlled environment the tribometer has an acrylic enclosure and attached valves which brings inert and other gases. Humidity levels can be control by an optional humidifier and dehumidifier module. There is also an oven available for rotative test up to 900°C and also heating plate is used for the linear test up to 300°C. Tests can either be performed under full absorption in a cup or using the lubrication system with drop by drop or control spray. A liquid heating module is also usable to provide controlled liquid heating up to 150°C. To quantify wear loss in a fast and convenient method without sample removal a full 3D non-contact optical profiler integrated on tribometer platform is available for that so as to precisely measure wear track volume. A tribometer software **figure 2.2** (b), uses this information and the test parameters to compute a precise wear rate for the specific examination. Surface topography measurement including roughness can be measured with the help of the profiler. Rotative Mode (ASTM G99): A test sampleis loaded with a flat, pin or ball to create a circular wear track as the bottom rotates with a precisely known weight and at a specific position from the center. The deflection of the direct load cell during the test determined the friction coefficient. The volume of material lost during the test are used to calculated the wear rates for the pin and the disk. The software allows change of friction at any specific point along one lap to be plotted versus time. The mass of the steel sample is measured before and after the wear test so as to know the mass loss of the samples [51].

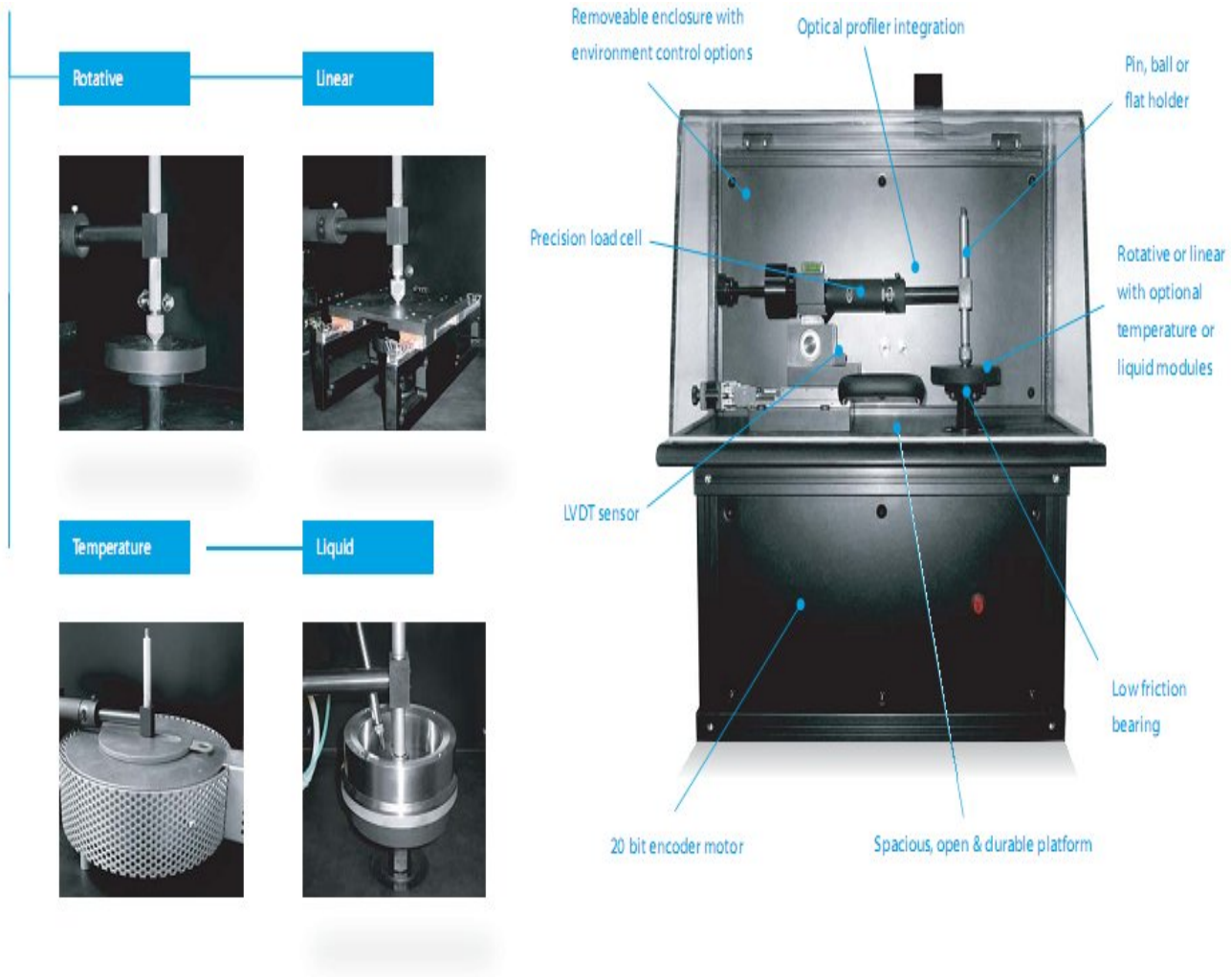

Figure 2.1 (a) s Nanoveatribometer.

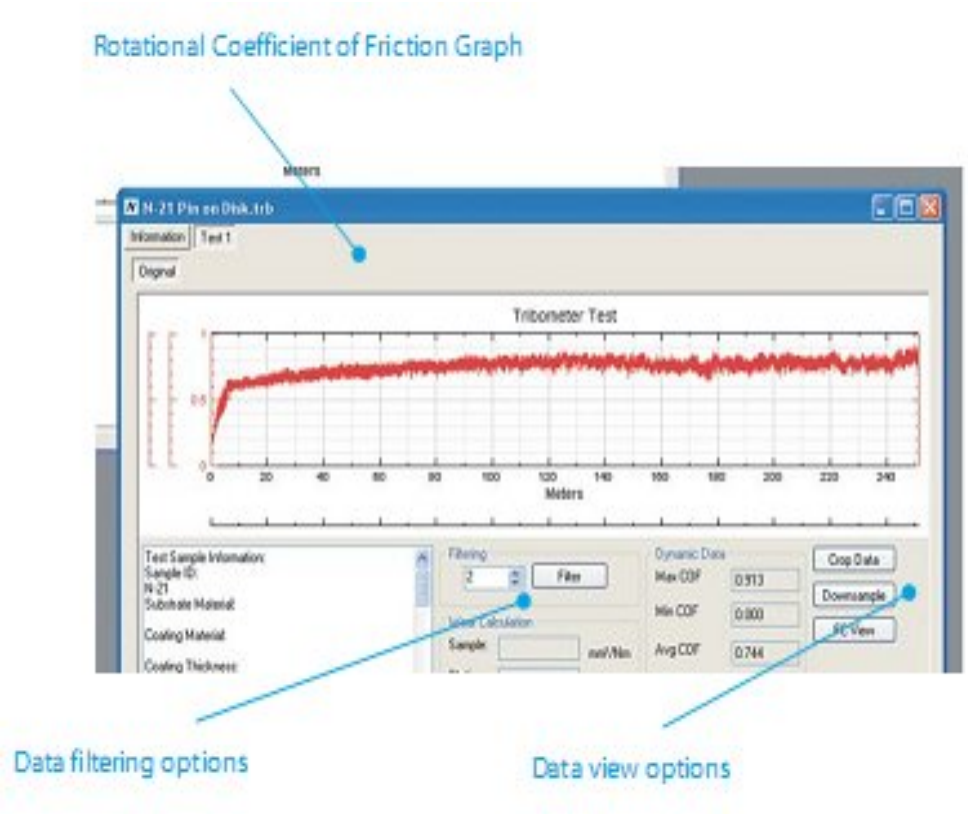

Figure 2.1 (b) an example wear from the Nanovea tribometer software.

2.3 EXPERIMENTAL PROCEDURE

2.3.1 Heat Treatment

2.3.2.1 Normalization

The specimen was first cut by a cutting machine as received in to small pieces and then put into a furnace for austenization at austenizing temperatures of 850^0C,860^0C, 880^0C,900^0C,960^0C and 1000^0C and held each at 40 minutes to dissolve the precipitates. And then the specimen was slowly cooled in atmosphere to room temperature so as to enable the formation of pearlite and ferrite. After that the specimen was mounted and then grinded and polished on a grinding machine to enable examination of the morphology and other mechanical properties.

2.3.2.2 Oil Quenching

The specimen was first cut by a cutting machine as received into small pieces and then put into a furnace for austenization at austenizing temperatures of 850^0C,860^0C, 880^0C,900^0C,960^0C and 1000^0C and then held each at 40 minutes to dissolve the precipitates. After then the specimen was fastly cooled in an oil to room temperature so as to enable the formation of martensite.Then, the specimen was placed in a mounting machine and then ground and polished on a grinding machine to enable examination of the morphology and other mechanical properties.

2.3.1.3 Water Quenching

The specimen was first cut by a cutting machine as received into small pieces and then put into a furnace for austenization at austenizing temperatures of 850^0C,860^0C, 880^0C,900^0C,960^0C and 1000^0C and held each at 40 minutes to dissolve the precipitates. And then the specimen was fastly cooled in water to room temperature so as to enable the formation of martensite. After that the specimen was mounted in a mounting machine and then grinded and polished on a grinding machine to enable examination of the morphology and other mechanical properties.

2.3.2 Wear Testing

After the specimen was ground, polished and etched to see the microstructure the specimen was the re-polished for wear testing so as to enable an accurate result. The mass of each specimen was then measured before and after the wear test so as to know the amount of mass loss during the wear testing process as a result of abrasive wear of the surface of the samples. The wear testing was carried at a sliding distance of 500m at 150rpm with a normal force of 10N in a rotative mode with a ball.

CHAPTER 3
EXPERIMENTAL RESULTS AND DISCUSSION

3.1 MICROSTRUCTURES OF INVESTIGATED STEEL

3.1.1 Optical Microscopy

The samples were grinded and polished in the standard manner for the basic metallographic characterization. The polished samples were etched with 5% nital to reveal the microstructures and they was taken by using the optical microscope.

A series of representative microstructure were taken on the grinded surface of each specimen at 200X magnification. Figure3.1 shows the microstructure for austenitizing temperature of 1000^{o}C in holding time of 40 minutes for the normalize specimen cooled in air. Under the present etching condition, ferrite or pearlite appears as brown, bainite appears as black, martensite appears as dark brown and carbide appears as a very bright island. Figure 3.1(a) is the microstructure of specimen 11(2.1ppm) obtained at 1000^{0}C for holding time of 40 minutes, and exhibited mainly a ferrite pearlite structure with little amount of bainite and martensite structures and some carbides. The prior austenite grain boundaries are covered by the carbides and upper bainite, and are hardly seen. The microstructure presented in figure 3.1 (b) has the same structure as figure 3.1 (a) except for the grain growth. The microstructure presented in figure 3.1 (c) shows a plane morphology and the microstructure in figure 3.1(d) shows much amount of ferrite in light color and pearlite in dark brown color with little amount of bainite in black color and also it shows little formation of carbide and clear austenite grain boundaries. Figure 3.1 (e) shows a high amount of ferrite and pearlite with less formation of carbide and negligible amount of bainite and martensite but with no grain boundaries and small grain size. Figure 3.1(f) shows ferrite and pearlite with much dark etched surface with needle like macrostructure.

In some areas, the darker phase starts to form in certain directions, which made this microstructure to have a more plate-like morphology. It is hard to tell based on the optical in microstructures what these darker-etched phases are. Microscopy with a higher resolution has to be used for characterizing the detailed features of these microstructures like SEM.

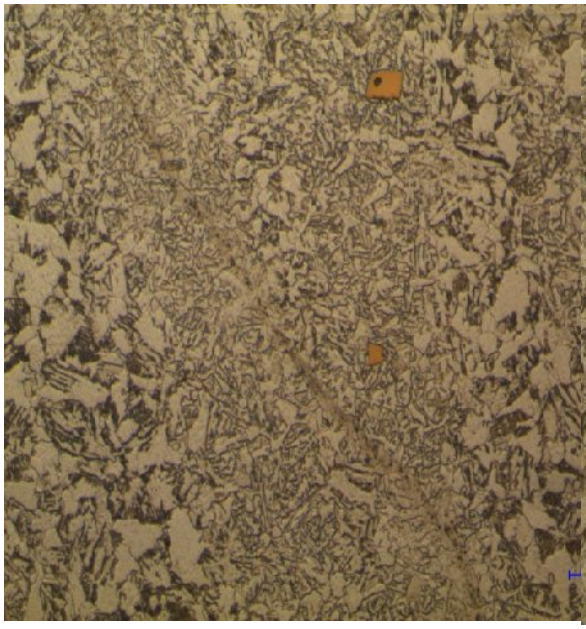

(a) N4140 11 1000^0C 40 minutes

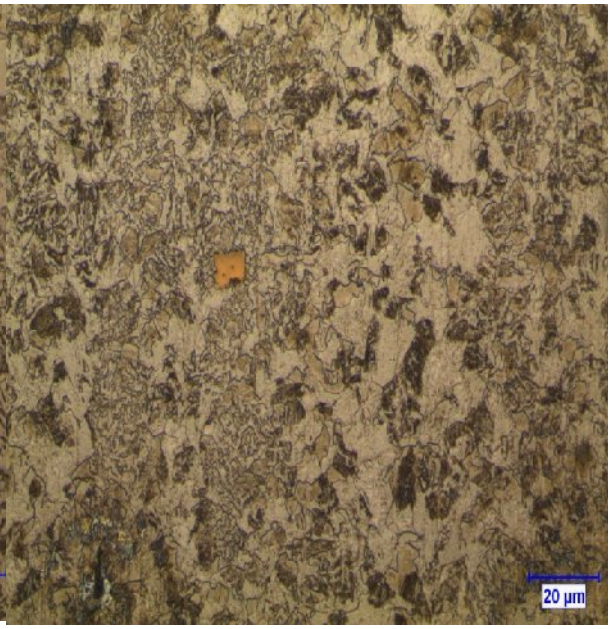

(b)N4140 12 1000^0C 40 minutes

(c) N4140 13 1000^0C 40 minute

(d) N4140 14 1000^0C40 minute

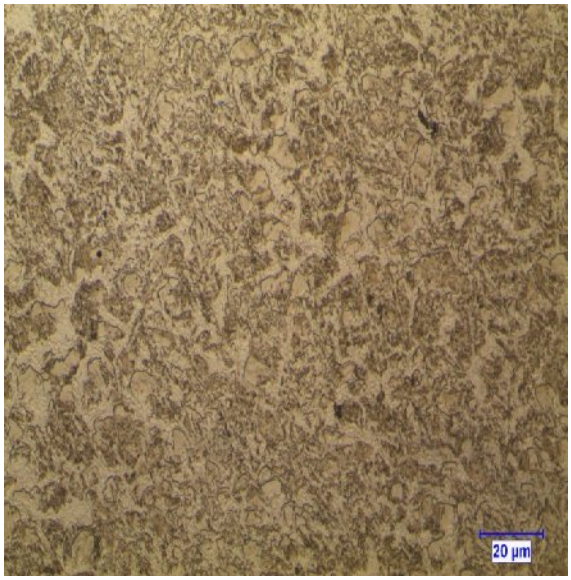

(e) N4140 15 1000^{0}C 40 minute

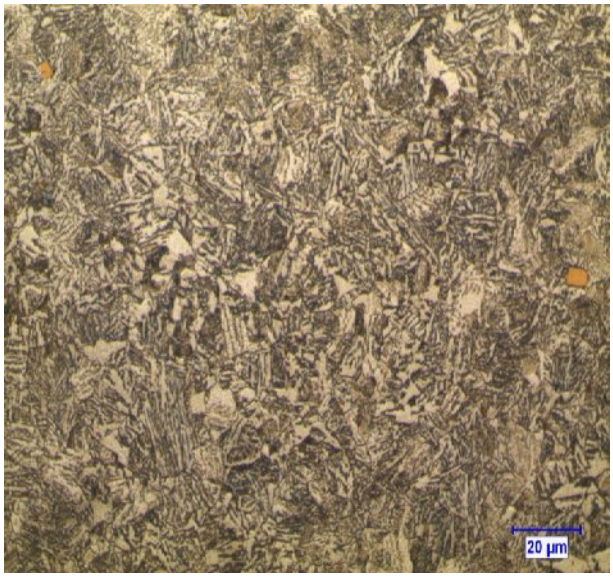

(f) N4140 16 1000^{0}C 40 minute

Figure 3.1 (a)-(f) the microstructures for 1000^{o}C austenitizing temperature for holding time of 40 minutes for the normalized air cooled specimen.

The formation of bainite and martensite in figure 3.1 is due to the addition of boron to the steel which does not affect the bainitic and martensite region, but affect the ferritic region as can be seen in figure 1.5. The ferrite region is shifted to the right while the bainite region to the left, which makes the cooling path to touches the bainite and martensite phase except in the case of annealing. The formation of carbide in the macrostructures is due to the precipitate behavior of boron in the solution.

Figure.3.2 shows the micrographs for austenitizing temperature of 1000^{o}C in holding time of 40 minutes for the water quenched specimen. Under the present etching condition, martensite or bainite appears as dark brown and black, and carbide appears very bright. Figure3.2 (a) is the microstructure of specimen 11(2.1ppm) obtained at 1000^{0}C for holding time of 40 minutes, and exhibites mainly a martensite structure with little amount of bainite and some carbides with plate like microstructure. The microstructure presented in figure 3.2 (b) has same structure as figure 3.2 (a) but with little retained austenite. The microstructure presented in figure 3.2(c) shows almost a plane morphology of martensite, and the microstructure in figure 3.2 (d) shows martensite and presence of some carbide. Figure 3.2

(e) shows a bright morphology of martensite. Figure 3.2 (f) shows bigger grain size of martensite, some carbide and little retained austenite. In some areas, the darker phase starts to form in certain directions, which made this microstructure to have a more plate-like morphology. It is hard to tell based on the optical micrographs what these darker-etched phases are, microscopy with a higher resolution has to be used for characterizing the detailed features of these microstructures like SEM.

(a)W4140 11 1000^{0}C 40

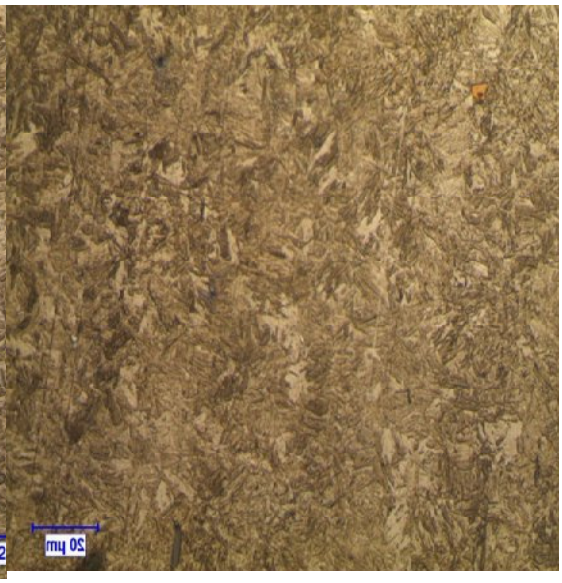

(b)W4140 12 1000^{0}C 40

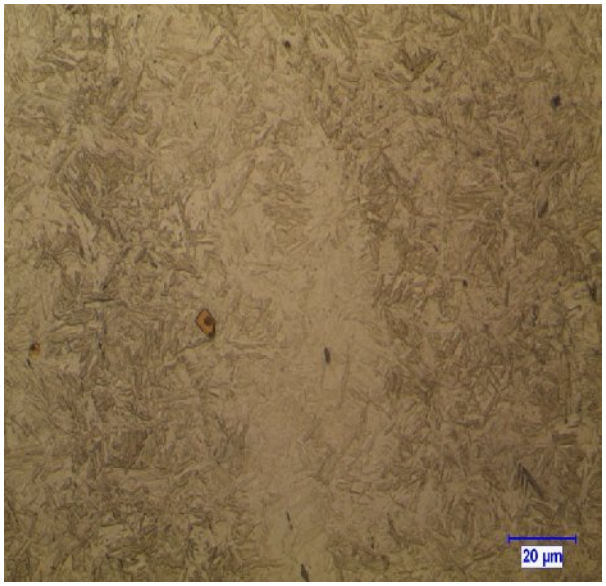

(c)W4140 13 1000^{0}C 40

(d)W4140 14 1000^{0}C 40

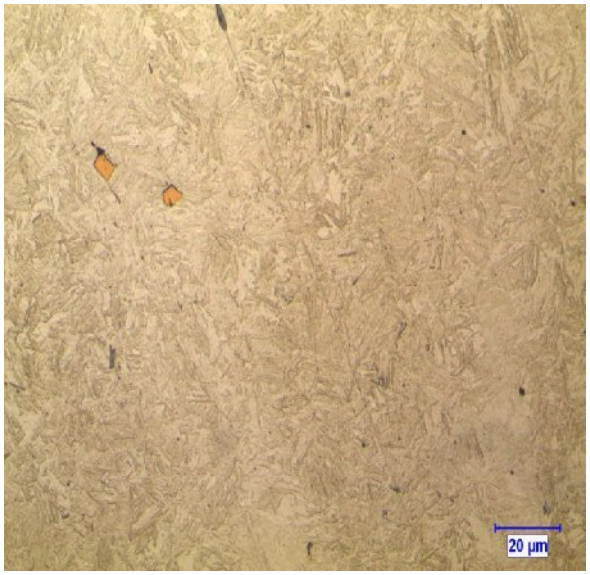

(e) W4140 15 1000^{0}C 40

(f)W4140 16 1000^{0}C 40

Figure 3.2 (a) -(f) The optical micrographs for 1000^{o}C austenitizing temperature for holding time of 40 minutes for the water quenched specimen.

The formation of bainite and martensite without ferrite in figure 3.2 is due to the addition of boron to the steel which does not affect the bainitic and martensite region but affect the ferritic region as can be seen in figure 1.5. The ferrite region is shifted to the right while the bainite region to the left which makes the cooling path to touches only the bainite and martensite phase. The formation of carbide in the macrostructures is due to the precipitate behavior of boron in the solution.

Figure 3.3 shows the microstructures for austenitizing temperature of 1000^{o}C in holding time of 40 minutes for the oil quenched specimen. Under the present etching condition, martensite and bainite appears as dark brown and black, and carbide appears very bright with retained austenite appearing as white. Figure 3.3 (a) is the microstructure of specimen 11(2.1ppm) obtained at 1000^{o}C for holding time of 40 minutes, and exhibited mainly a martensite structure with little amount of bainite and some carbides with plate like microstructure. The microstructure presented in figure 3.3 (b) has the same structure as figure 3.3 (a) but with almost a plane morphology. The microstructure presented in figure3.3(c)

shows martensite, and the microstructure in figure 3.3 (d) shows martensite and bainite with retained austenite. Figure 3.3 (e) shows a much black etched structure of bainite and martensite with no retained austenite. Figure 3.3(f) shows martensite and some carbide. In some areas, the darker phase starts to form in certain directions, which made this microstructure to have a more plate-like morphology. It is hard to tell based on the optical micrographs what these darker-etched phases are. Microscopy with a higher resolution has to be used for characterizing the detailed features of these microstructures like SEM.

(a) Q4140 11 1000^{0}C 40

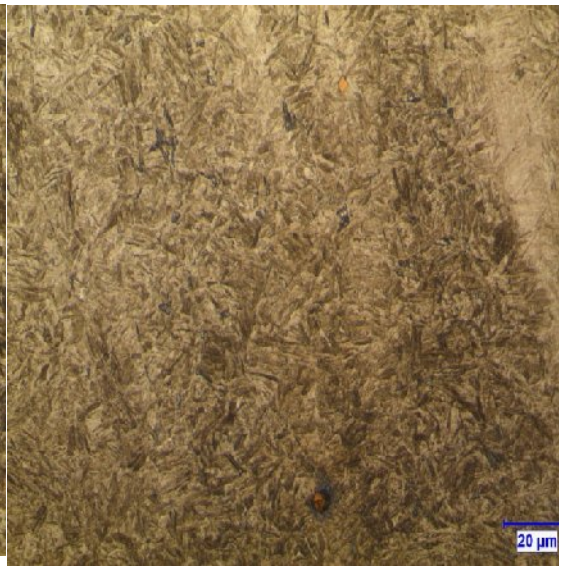

(b)Q4140 12 1000^{0}C 40

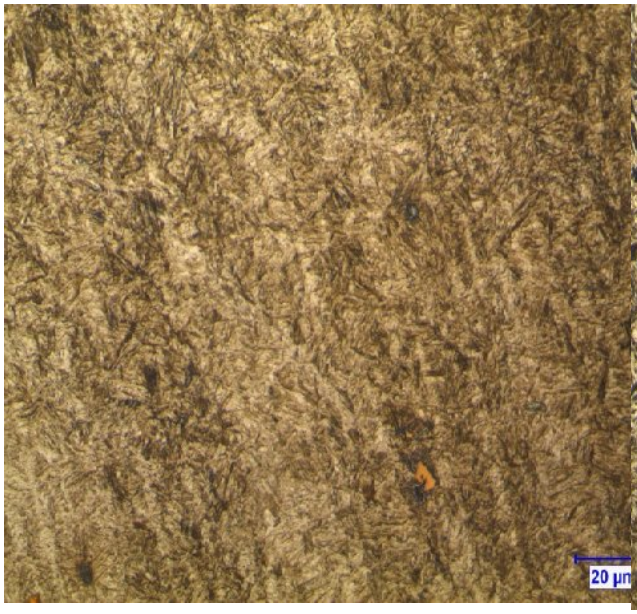

(c)Q4140 13 1000^{0}C 40

(d)Q4140 14 1000^{0}C 40

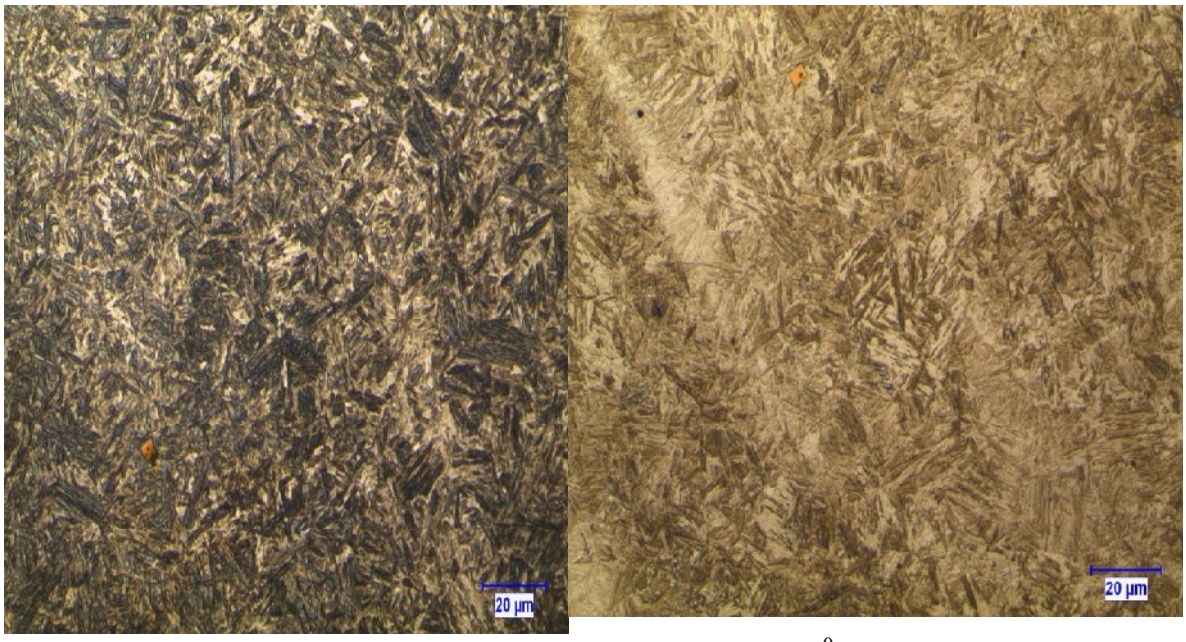

(e) Q4140 15 1000^0C 40 (f) Q4140 16 1000^0C 40

Figure 3.3 (a)-(f) the optical micrographs for 1000°C austenitizing temperature for holding time of 40 minutes for the oil quenched specimen.

The formation of bainite and martensite without ferrite in figure 3.3 is due to the addition of boron to the steel which does not affect the bainitic and martensite region but affect the ferritic region as can be seen in figure 1.5. The ferrite region is shifted to the right while the bainite region to the left which makes the cooling path to touches only the bainite and martensite phase. The formation of carbide in the macrostructures is due to the precipitate behavior of boron in the solution.

3.2 MECHANICAL PROPERTIES

3.2.1 Results for Hardness Testing

Table 3.1, 3.2 and 3.3, figures 3.4, 3.5 and 3.6 show the results of hardness test values and each with its graphs obtained at various temperature for different cooling methods. The results show that, higher hardness is obtained in the water quenching compare to oil

quenching because of the rapid cooling in water compared to oil and much less hardness in air cooling because of the low cooling rate which enhances the formation of ferrite and pearlite.

3.2.1.1 Normalization

It can be seen from figure 3.4 (a) that the hardness starts increasing as the boron content increases up to 17.5ppm, except for T860 and T900 but drops at the highest boron content with the maximum and minimum hardness at 17.5 and 31.7ppm. In figure 3.4 (b), it is seen that hardness of steels,s1 and s3 decrease as the temperature increase up to 900^0C and later increase at 960^0C but decrease at 1000^0C. The minimum hardness is observed in steel s5 and s6 at 960^0C which later increase at 1000^0C. The decrease and increase in the hardness of the steel is due to the phase transformation and precipitation behavior of boron [49].

This decrease and increase of hardness in this steel is as a result of the precipitate behavior of boron, which is caused as a result of increase in the amount of ineffective boron in the steel and also as a result of increasing austenitizing behavior and cooling conditions.

Table 3.1 HRC Normalize and as received (AR) hardness values

HRC Normalize and as received(AR) hardness values						
Boron content	**2.1ppm**	**11.4ppm**	**17.2ppm**	**25.6ppm**	**31.7ppm**	**37.7ppm**
AR	**28.83**	**27.55**	**26.95**	**28.18**	**24.18**	**23.93**
850^0C	**40.3**	**42.5**	**43.9**	**44.6**	**44.4**	**34.4**
860^0C	**32.3**	**44.6**	**40.7**	**43.2**	**42.2**	**41.0**
880^0C	**34.7**	**42.6**	**43.0**	**41.5**	**42.1**	**40.1**
900^0C	**30.6**	**44.9**	**42.5**	**42.5**	**37.0**	**40.8**
960^0C	**41.3**	**41.6**	**45.8**	**41.6**	**23.60**	**30.0**
1000^0C	**29.2**	**39.8**	**42.08**	**41.5**	**39.1**	**35.9**

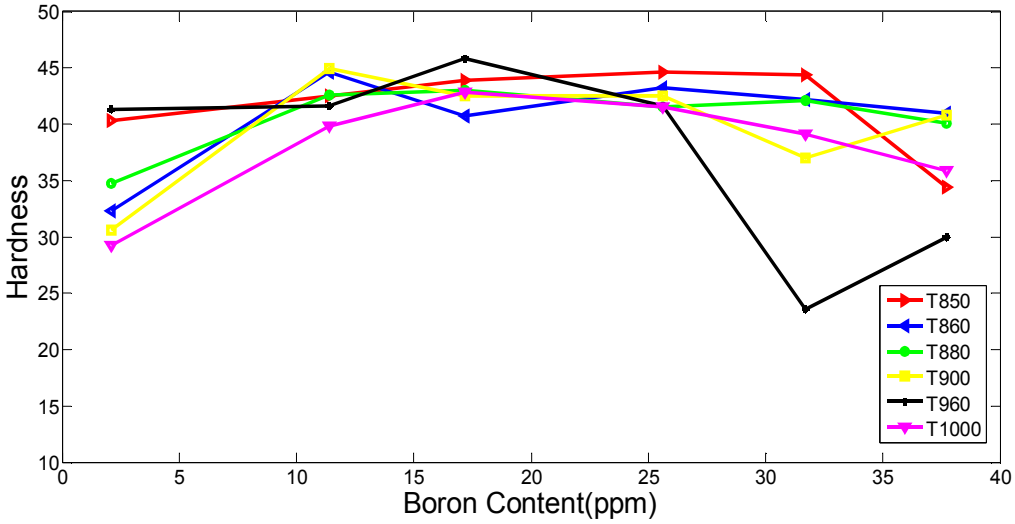

Figure 3.4 (a). The graph of normalization hardness against boron content

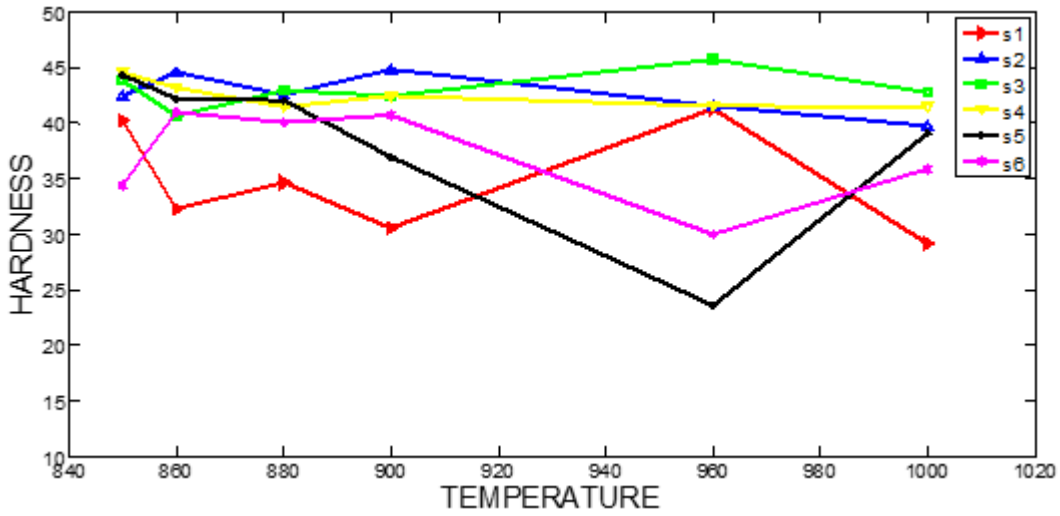

Figure 3.4 (b) the graph of normalization hardness against temperatures

3.2.1.2 Oil Quenching

In this cooling method it can be seen in figure 3.5 (a) that the hardness value increases with increase in boron content except for T850 and T860 which is fluctuating. In figure 3.5 (b) it can be seen that for 2.1 and 11.4 ppm boron content steel the hardness values decreases as the temperature increases while 17.2 and 37.7 ppm increases at first up till 880^{0}C and then

decreases as the temperature increases. Also 25.6 and 31.7 ppm decreases as the temperature increase to 860^0C and then increase at 880^0C which later decrease up to 1000^0C.The decrease and increase in the hardness of the steel is due to the phase transformation and precipitation behavior of boron.

This fluctuation of hardness in this steel is as a result of the precipitate behavior of boron, which is caused as a result of increase in the amount of ineffective boron in the steel and also as a result of increasing austenitizing behavior and cooling condition.

Table 3.2HRC Oil quenching hardness value

HRC Oil quenching hardness value						
Boron content	2.1ppm	11.4ppm	17.2ppm	25.6ppm	31.7ppm	37.7ppm
1000^0C	50.4	51.43	51.5	50.57	53.0	53.83
960^0C	55.4	54.2	55.53	54.9	54.1	54.6
900^0C	56.1	55.9	56.23	56.4	56.33	55.6
880^0C	56.83	57.1	57.0	56.53	56.67	56.77
860^0C	56.9	57.43	51.03	51.1	47.37	53.67
850^0C	56.43	47.73	50.2	56.97	56.17	50.4

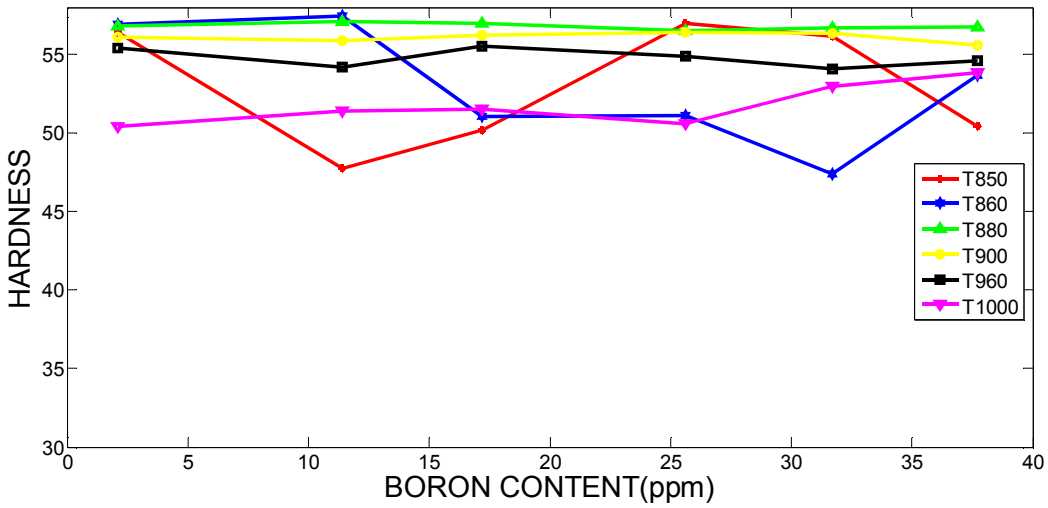

Figure 3.5 (a) the graph of oil quenching hardness against boron content.

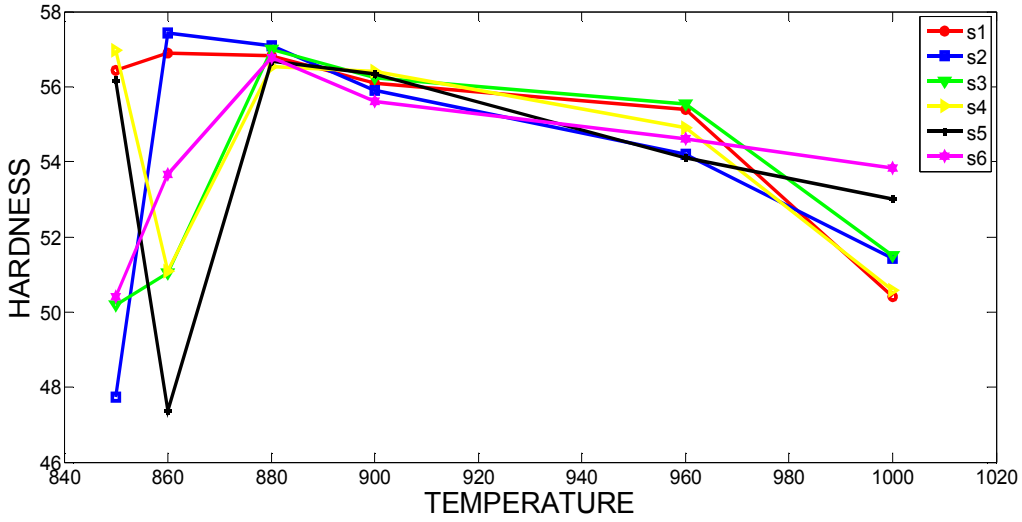

Figure 3.5 (b) the graph of oil quenching hardness against temperature.

3.2.1.3 Water Quenching

In this quenching method it can be seen in figure 3.6 (a) that in T850 and T960 they is an increment in the hardness value as the boron content increases while T880 decreases as the boron content increases. In T860 and T900 they is a fluctuation of decrement and increment as the boron content increases. In T1000 it decreases as the boron content increases except at the boron content of 25.6 and 31.7ppm.

In figure 3.6 (b) it can be seen that the hardness value decrease in 37.7ppm (s6) steel as the temperature increases except at 960^0C. In 2.1ppm (s1) steel the hardness value increase up to 880^0C and then decreases as the temperature continue to increase. In 11.4ppm (s2) steel the hardness value decreases first and then increase at 880^0C which in turn continue to decease as the temperature increase. In 17.2ppm (s3) steel the hardness value decreases at first and then increase at 900^0C which later decrease again as the temperature increases. In 25.6ppm (s4) steel the hardness value decreases and then start increasing at 900^0C. In 31.7ppm (s5) steel they is a fluctuation of decrement and increment in the hardness value as the temperature increases. The fluctuation in the hardness of the steel is due to the phase transformation and precipitation

This fluctuation of hardness in this steel is as a result of the precipitate behavior of boron, which is cause as a result of increase in the amount of ineffective boron in the steel and also as a result of increasing austenitizing behavior and cooling condition.

Table 3.3HRC Water quenches hardness value

HRC Water quenches hardness value						
Boron content	2.1ppm	11.4ppm	17.2ppm	25.6ppm	31.7ppm	37.7ppm
850^0C	58.1	58.5	58.8	58.83	57.87	59.1
860^0C	59.2	58.33	58.73	58.23	58.67	58.6
880^0C	59.33	58.83	58.7	58.23	58.2	58.5
900^0C	58.73	58.57	58.87	58.6	58.77	58.27
960^0C	55.4	55.67	56.17	58.77	57.47	58.53
1000^0C	56.73	55.9	54.3	55.3	56.47	54.8

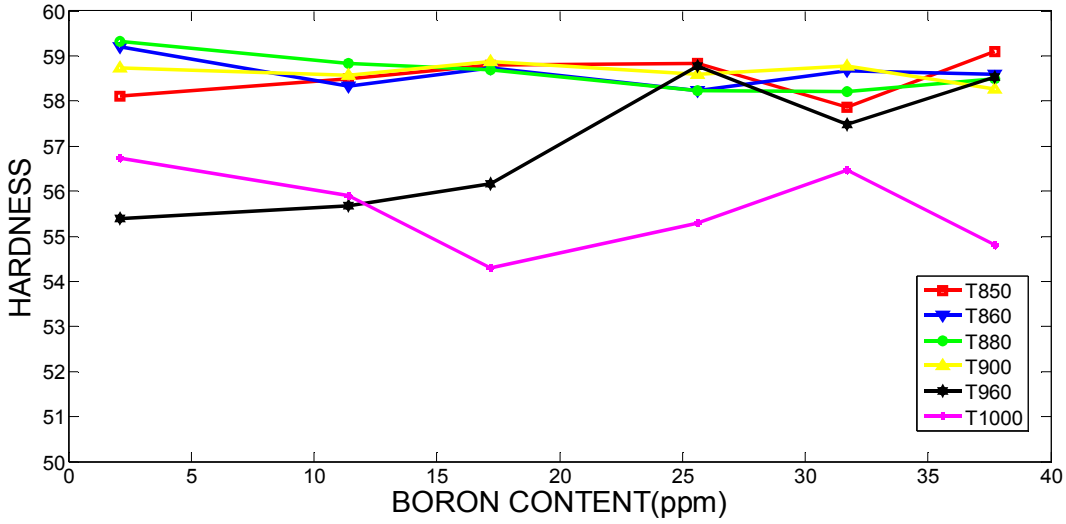

Figure. 3.6(a) The graph of water quenching hardness against boron content.

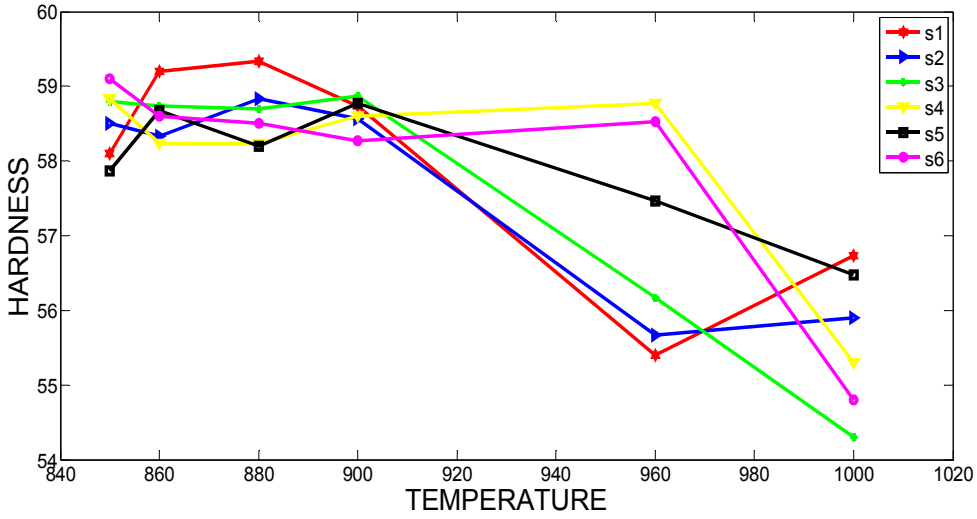

Figure 3.6 (b) the graph of water quenching hardness against the temperatures.

Figure 3.7 (a) Shows the comparison of the different heat treated steel and the steel as received at 1000ºC austenizing temperature. It can be seen that the as-received steel has the minimum hardness and the water quench has the maximum hardness which is about twice the amount of hardness as received, because of the high amount of martensite formation due to the boron effect. Also, it can be seen that the hardness changes with increase in boron content, but not uniform due to the phase transformation and precipitate formation.

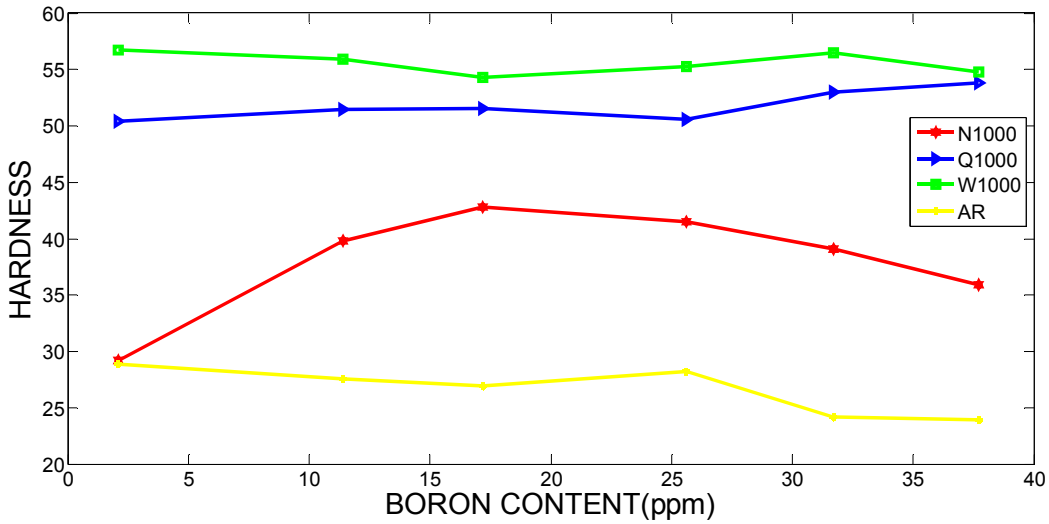

Figure 3.7 (a) the comparison graph for as received and the heat treated steel hardness values against boron content at 1000ºC.

Figure 3.7 (b) shows the comparison of the different heat treated method for different austenizing temperature for the steel with 17.6ppm boron content. It can be seen that the steel in the normalized cooling method (Ns3) has the minimum hardness whereas the water quench has the maximum hardness because of the high formation of martensite due to the boron effect. Additionally, it can be seen that the hardness changes with increase in boron content, but not uniform due to the phase transformation and precipitate formation.

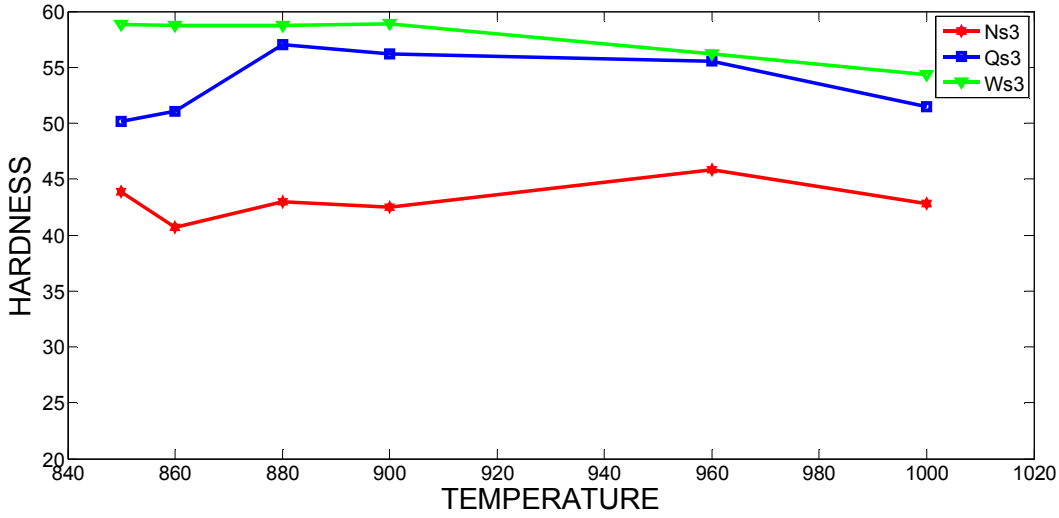

Figure 3.7 (b) the comparison graph for as-received and the heat treated steel hardness value against temperature for steel s3 (17.6 ppm boron content).

3.2.2 Results of Wear Testing

3.2.2.1 Mass Loss for Each Test

Table 3.4 shows the mass loss of the wear test for steel with six different boron content after 500m sliding distance at the rate of 150rpm with the normal load of 10N.

In figure 3.8, it can be seen that the mass loss in the steel as-received (AR) is comparatively higher than the heat treated steels because of the low hardness value of the steel as received to the heat treated steels. The mass loss of the normalized steels is higher than the mass loss of the quenched steel but lower than the mass loss of the steel as-received. The mass loss of the oil quenched steel is higher than the water quenched but lower than the

air cooled and the as-received steel. Additionally, the mass loss of the oil and water quenched steel at1000^0**C** is higher than the oil and water mass loss at 960^{0}C because temperature plays a very important role in the hardenability of a steel. This reason makes the mass loss to be different for same steel with same boron content in same cooling method but with different austenitizing temperature.

Table 3.4 Mass loss in gram (g)

Mass loss in gram(g)						
	2.1ppm	11.4ppm	17.2ppm	25.6ppm	31.7ppm	37.7ppm
N1000	0.0049	0.0039	0.0035	0.0038	0.0039	0.0034
N960	0.0032	0.0038	0.0036	0.0039	0.0053	0.0043
Q1000	0.0037	0.0032	0.0025	0.0031	0.0030	0.0024
Q960	0.0023	0.0024	0.0021	0.0019	0.0031	0.0026
W1000	0.0019	0.0028	0.0029	0.0026	0.0017	0.0033
W960	0.0023	0.0021	0.0024	0.0019	0.0022	0.0017
AR	0.006	0.0056	0.0062	0.0078	0.0084	0.0096

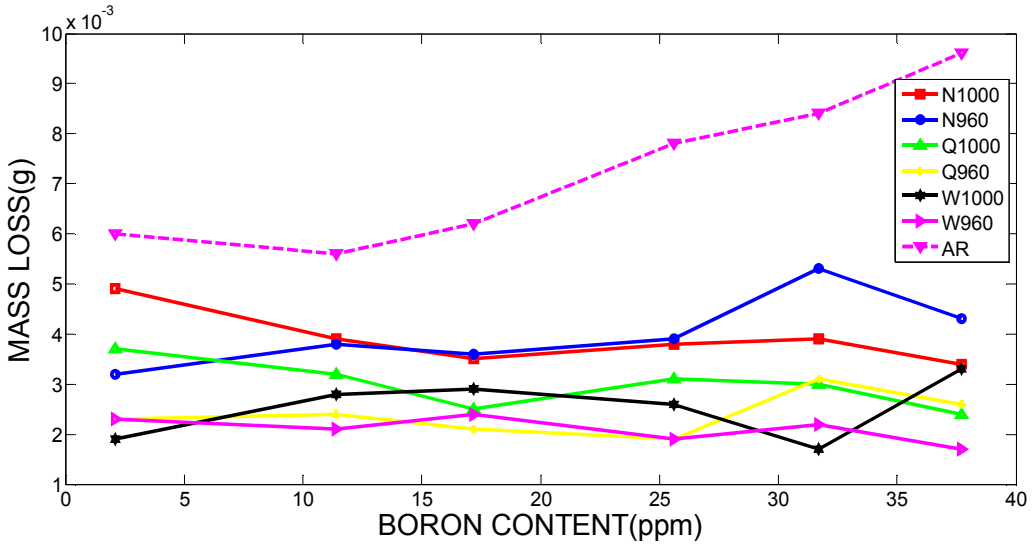

Figure 3.8 The amount of mass loss against boron content

3.2.2.2 Comparison between Coefficient Of Friction for As-Received State and Heat Treated Method at 960^{O}C and 1000^{O}C.

The mass loss decreases with increasing boron content in the steel as-received, but scatter in the heat treated steels due to boron precipitation behavior which depends on austenitizing temperature and cooling conditions.

Comparison between coefficient of friction against sliding distance for as-received state, oil quenched Q4140 and water quenched W4140 cooling method in steel 12(11.4 ppm boron content) at 960^{O}C and 1000^{O}C with 40 minutes holding time are shown in figure 3.9. For the wear testing, a normal force (F_N) of 10N is used. The coefficient of friction varies because of the differences in the hardness of the steel, with the as-received state having maximum coefficient of friction of 0.779. For the normalized steel sample the maximum coefficient of friction is 0.629 at 960^{O}C and 0.558 at 1000^{O}C. For the oil quenched steel sample the maximum coefficient of friction is 0.641 at 960^{O}C and 0.741 at 1000^{O}C. For the water quenched steel sample the maximum coefficient of friction is 0.541 at 960^{O}C and 0.730 at 1000^{O}C.

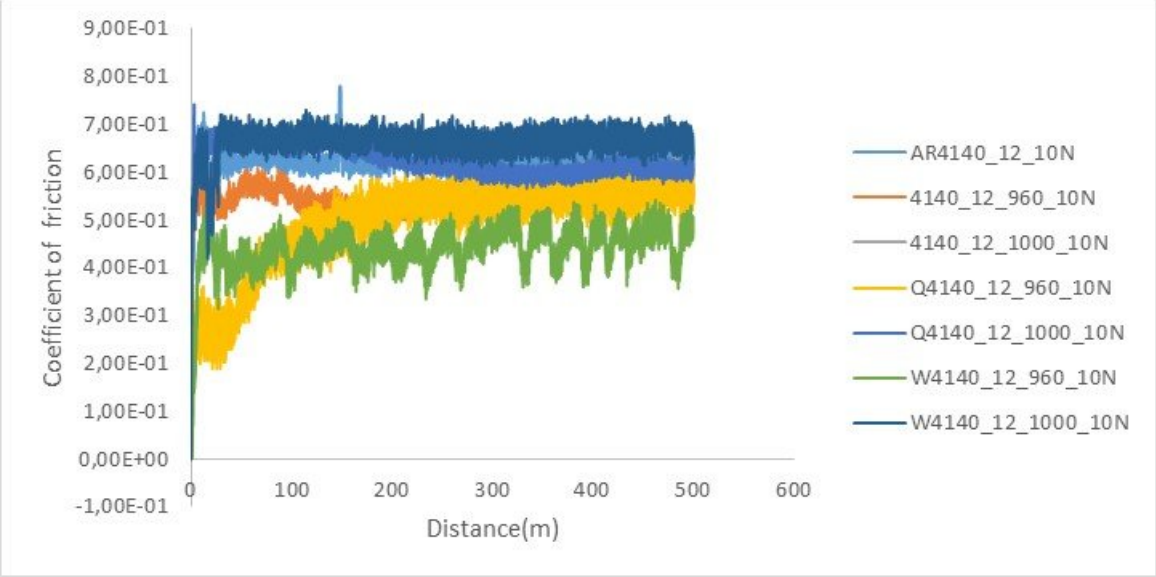

Figure 3.9 The graph of coefficient of friction against sliding distance for as-received state, oil quenched (Q4140) and water quenched (W4140) method in steel 12 (11.4 ppm boron content) at 960^{O}C and 1000^{O}C.

Comparison between coefficient of friction against sliding distance for as-received state, oil quenched Q4140 and water quenched W4140 cooling method in steel 11(2.1 ppm boron content) at 960^{O}C and 1000^{O}C, with 40 minutes holding time are shown in figure 3.10. For the wear testing a normal force (F_N) of 10N is used. The coefficient of friction varies because of the differences in the hardness of the steel, with the as-received state having maximum coefficient of friction of 0.701. For the normalized steel sample the maximum coefficient of friction is 0.582 at 960^{O}C and 0.631 at 1000^{O}C.For the oil quenched steel sample the maximum coefficient of friction is 0.715 at 960^{O}C and0.803 at 1000^{O}C.For the water quenched steel sample the maximum coefficient of friction is 0.604 at 960^{O}C and0.721 at 1000^{O}C.

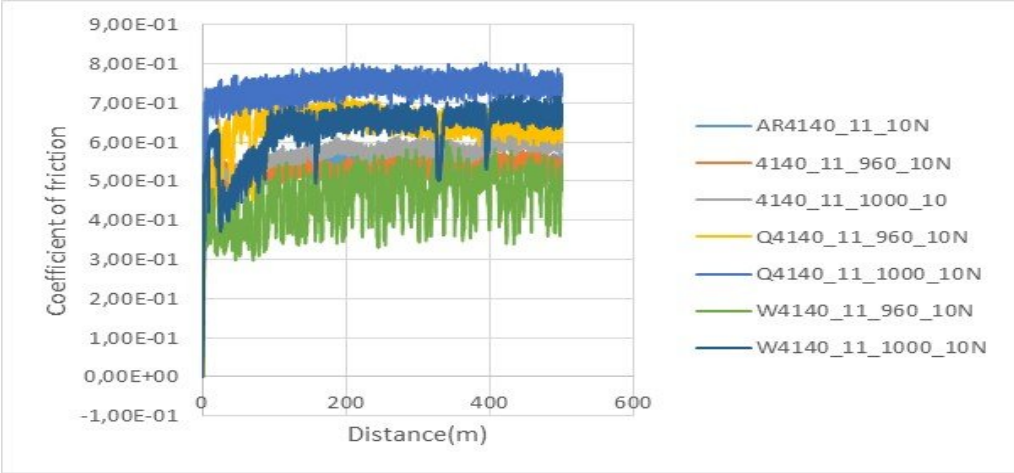

Figure 3.10 The graph of coefficient of friction against sliding distance for as-received state, oil quenched (Q4140) and water quenched (W4140) method in steel 11 (2.1 ppm boron content) at 960^{O}C and 1000^{O}C

From figure 3.11 it can be seen that steel 15 (31.7ppm) has the highest coefficient of friction and steel 12 (11.4) has the lowest coefficient of friction. The coefficient of friction increases as the boron content increase up to 31.7ppm (15) except for the steel with boron content 2.1ppm (11) and 37.7ppm (16). The decreasing and increasing of the coefficient of friction with increasing boron content is due to boron precipitation behavior

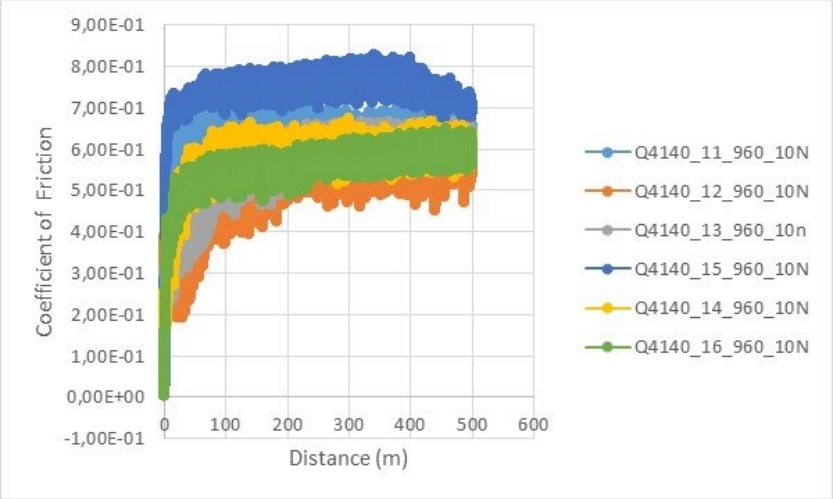

Figure 3.11 The graph of Coefficient of friction against sliding distance with different boron content for oil quenched (Q4140) method at 960^{O}C.

Table 8: Wear Test Results

Designation	Max. Frictional Force (N)	Max. Coeff. Friction	Time (Min.)	Distance (m)	Normal Force (N)
AR_11_10N	7.015	0.785	212.314	500	10
N4140_11_1000^{O}C	6.308	0.631	212.314	500	10
N4140_11_960^{O}C	5.816	0.582	212.314	500	10
Q4140_11_1000^{O}C	8.033	0.803	212.314	500	10
Q4140_11_960^{O}C	7.149	0.715	212.314	500	10
W4140_11_1000^{O}C	7.212	0.721	212.314	500	10
W4140_11_960^{O}C	6.043	0.604	212.314	500	10
AR_12_10N	7.787	0.612	212.314	500	10
N4140_12_1000^{O}C	4.281	0.558	212.314	500	10
N4140_12_960^{O}C	6.268	0.627	212.314	500	10
Q4140_12_1000^{O}C	7.4114	0.741	212.314	500	10
Q4140_12_960^{O}C	6.415	0.641	212.314	500	10
W4140_12_1000^{O}C	7.296	0.730	212.314	500	10
W4140_12_960^{O}C	5.412	0.541	212.314	500	10

Table 8 shows the wear test result, which shows how the frictional force and coefficient of friction are affected with different heat treatment and different quenching medium with different austenitizing temperature.

CHAPTER 4

CONCLUSIONS

Boron doped AISI 4140 steel was investigated in this research work to obtain the microstructural and mechanical effect of boron addition, after some of heat treatment processes, normalization and quenching in different medium such as oil and water, comparison has been done with those of as received steels. The main results of the study can be summarized as follows;

1. The microstructure of all the steel after normalization shows no grain boundaries because of too much carbide precipitate and upper bainite formation except for the steel with 25.6 ppm boron content. The microstructure for the oil quenched steel shows martensite with little amount of retained austenite and the microstructure for the water quenched steel shows very little or no retained austenite.

2. It is observed that boron content less than 0.0008%, as low as 2.1ppm increases the hardness of AISI 4140 steel significantly. And the hardness values in this steel doesn't make much difference as the boron content increases. Additionally, it was also observed that there is little difference in the hardness values as the temperature increase from 850^{o}C to 960^{o}C but rather fluctuate. This fluctuation of hardness in this steel is as a result of the precipitate behavior of boron, which is cause as a result of increase in the amount of ineffective boron in the steel and also as a result of increasing austenitizing behavior and cooling condition.

3 The mass loss decreases with cooling condition and temperature, with the highest amount of mass loss observed in the steel as-received and the least in the water and oil quenched steel at 960^{o}C because of the effect of temperature and cooling condition on hardness value.

4. The mass loss decreases with increasing boron content in the steel as-received, but scatter in the heat treated steels due to boron precipitation behavior which depends on austenitizing temperature and cooling condition.

5. The coefficient of friction decreases with cooling conditions and increase temperature, but fluctuate with increasing boron content due to boron precipitation behavior.

REFERENCES

1. P.D. Deeley, K.J.A. Kundig, *Review of Metallurgical Applications of Boron Steels,* Shieldalloy Corporation, Newfield, New Jersey.

2. T.W. Lippert, Boron, *the Iron Age,* Nov. **19,** 1942.

3. R. Walter, British Patent160, 792, 1921; U.S. Patentl,519,388, Aug. 13, 1921.

4. M.A. Grossman, *Trans.* AIME, 150, pp. 227, 1942.

5. G.F. Comstock, *Trans.* AIME, 150, pp. 408, 1942.

6. R.A. Grange, Boron in Iron and Steel, Boron, Calcium, Columbium and Zirconium in Iron and Steel Alloys of Iron, *Research Monograph Series*, John Wiley and Sons, Inc. N.Y., N.Y. pp. 3, 1957.

7. G.D. Rahrer, C.D. Armstrong, *Trans.* ASM, 40, pp.1099, 1948.

8. Anjana Deva, N.K.Jha, B.K.Jha *International Journal of Metallogical Engineering on*Effect of austenitising temperature and cooling condition on mechanical properties of low carbon boron containing steel, 2012.

9. M. I.HAQ,NAZMA IKRAM *Journal of Material Science*The effect of boron addition on the tensile properties of control rolled and normaslized C – Mn steels, 28(1993)5981-5985.

10. A.A. Azarkevich, L.V. kovalenko, and V.M krasnopolskii *Journal of Material Science and heat treatment* The optimum content of boron in steel vol.37, No 1-2, 1995.

11. J. H. devletian and R. W Heine *Review on* Effect of boron content on carbon steel welds 1975.

12. Melloy, G.F., Slimmon, P.R. and Podgursky, P.P., 1973, "Optimizing the Boron Effect," J. of Metallurgical and Materials Transaction B, Vol. 4(10), pp. 22792289.

13. A. verma, K.gopinath*Journal of Engineering Research on* Boron steel: an alternative for costlier Nickel and molybdenum alloyed steel for transmission gears vol. 8 No.1(2011) 12-18.

14. B.M. Kapadia, R.M. Brown, W.J. Murphy, *Trans.* AIME, 242, pp.1689, 1968.

15. Ph. Maitrepierre, J Rofes-Vemis, D. Thivellier, *Boron in Steels,* S.K. Banerji, J.E. Morral, eds., AIME, p. 1, 1980.

16. Ph. Maitrepierre, D. Thivellier, J. Rofes-Vemis, D. Rousseau, R. Tricot, *Hardenability Concepts with Applications to Steel,* D. Doane, J.S. Kirkaldy, ed., AIME, p. 421, 1978.

17. H. Tamehiro, M. Murata, R. Habu, M. Nagumo, *Optimum Microalloying of Niobium* and *Boron in HSLA* Steel for Thermo mechanical Processing, Trans. ISIJ. Vol. 27, no. 2,pp. 120-129.1987.

18. B.J. Thomas, G. Henry, *Boron in Steels,* Proc. Int. Symp. On Boron Steels, eds.S.K. Banerji, J.E. Morral, TMS/AIME, p. 80, 1980.

19. D.J. Hayes, Proc. 14th Mechanical Working and Steel Processing Conference, Chicago, 1972.

20. M. Ueno and T. Inoue: *Trans. Iron Steel Inst. Jpn.,*13, pp. 210, 1973.

21. A. Brown, J. D Gamish and R. W. K. Honeycombe: *Met. Sei.,*8, pp. 317, 1974.

22. R. A. Grange and J. B. Mickel: *Trans. Am. Soc. Met.,* 53, pp.15, 71956.

23. G. F. Melloy, P. R. Slimon and P. P. Podgursky: *Metal/. Trans.,* 4, pp. 2279, 1973.

24. Y. Yamanaka and Y. Ohmori: *Trans. Iron Steel Inst. Jpn.,*17, pp. 92: 1977, 18, pp. 492, 1978.

25. R. Habu, M. Miyata and S. Sekino and S. Goda: *Trans. Iron Steel Inst. Jpn.,*18, 492, 1978.

26. M. Deighton, J. *Iron Steel Inst.,* 205, pp. 355, 1967

27. J.E. Morral, T.B. Cameron, *Boron Hardenability Mechanisms,* Boron in Steel, S.K. Banerji, J.E. Morral, eds.,TMS/AIME, p.19, 1980.

28. S.F. Urban and G.F. Comstock, U.S. Patent No. 2, 602, 028, 1952

29. S.K. Albert, M. Kondo, M. Tabuchi, F.X. Yin, K. Sawada, F. Abe, *Improving the Creep Properties of9Cr-3W-3Co-NbV Steels and their Weld Joints by the Addition of Boron,* Metallurgical and Materials Transactions, 36A, p. 333,2005.

30. N. Takahashi, T. Fujita, T. Yamanaka, Trans. ISIJ, 15, p. 438, 1975

31. R.C. Sharma, G.R. Purdy, *Metal!. Trans.,* 4A, p. 2303, 1973.

32. M. P. Seah, E. D. Hondros, *Inst. Met. Rev.* 222 p. 262, 1977.

33. D. McLean, "Grain boundaries in metals" (Clarendon Press, Oxford, 1957).

34. M. Guttman, *Met. Sei.* 10, p. 337, 1976.

35. J.H. Westbrook, *!nt. Metal!. Rev.,* 9, p.415, 1964.

36. T.R. Anthony, *Acta Metal!.*17, p. 603, 1969.

37. K. T. Aust, S. J. Armijo, E. F. Kock, J. A. Westbrook, *Trans. Amer. Soc. Metals* 60, p. 360, 1967.

38. S. Watanabe, H. Ohtani, T. Kunitake, *The Influence of Hot Rolling* and *Heat Treatments on the Distribution of Boron in Steel,* Trans. ISIJ., 23, no. 1, pp. 31-37. 1983.

39. S.H. Song, Z.X. Yuan, T.D. Xu, *Non-equilibrium segregation of boron at austenite grain boundaries,* Materials Science Letters, 10, pp. 1232-1234, 1991.

40. F.B. Pickering, *Microalloying 75,* Union Carbide Corporation, New York, p. 9, 1977.

41. Forging Knives The Cooling Path 2009. http://www.navaching.com/forge/cooling.html

42. R. Manna *Conference on* Time Temperature Transformation (TTT) Diagrams, Banaras Hindu University Varanasi-221 005, india.

43. FeMET Structural and Property of 4140 Austenitized Steel Quenched 2013http://femet.wsu.edu/Structure&PropertyA4140Q.html

44. N. Saunders, Z. Guo, X. Li, A.P. Miodownik, J.P. Schillé: The calculation of TTT and CCT diagrams for general steels, Internal report, Sente Software Ltd., U.K., 2004.

45. J.S. Kirkaldy, D.Venugopolan, in: Phase transformations in ferrous alloys, eds. A.R. Marder and J.I. Goldstein, AIME, (Warrendale, PA: AIME, 1984) 125.

46. Introduction of Materials Modelling into Processing Simulation – Towards True Virtual Design and Simulation ZhanliGuo, Nigel Saunders, A. Peter Miodownik, Jean-Philippe Schillé

47. Mechanical behavior of material second edition page 219

48. Hardness test methods*Dr. Dmitri Kopeliovich* http://www.substech.com/dokuwiki/doku.php?id=hardness_test_methods

49. Effect of Boron on Microstructure and Mechanical Properties of Low Carbon Microalloyed Steels Yu Lu McGill University Montreal, Canada June 2007

50. Cemal ÇARBOĞA, Burhanettin INEM and C. Sencer IMER, Journal paper on The Effect Of Hardening Heat Treatment On AISI 1022 Steel Containing 15 And 26 ppm Boron *Technology, 13(3), 139-144, (2010).*